GEORGIA INSTITUTE OF TECHNOLOGY
OFFICE OF CONTRACT ADMINISTRATION
SPONSORED PROJECT INITIATION

Date: January 7, 1977

Project Title: Comparative Evaluation of Woven-Graphite-Epoxy Composites

Project No: E-16-604

Project Director: Dr. S. V. Hanagud

Sponsor: National Aeronautics and Space Administration

Agreement Period: From 2/1/77 Until 1/31/78

Type Agreement: Grant No. NSG 1352

Amount: $19,994 NASA
2,998 GIT (E-16-380)
$22,992

Reports Required: Semi Annual Status; Final Technical Report

Sponsor Contact Person (s):

Technical Matters

Dr. Wolf Elber
Technical Officer
Materials Division
National Aeronautics and
Space Administration
Langley Research Center
Hampton, VA 23665
(804)827-3192

Contractual Matters
(thru OCA)

Mr. Frank S. Kawalkiewicz
Grants Officer
National Aeronautics and
Space Administration
Langley Research Center
Hampton, VA 23665
(804)827-3629

Defense Priority Rating: None

Assigned to: Aerospace Engineering (School/Laboratory)

COPIES TO:

- Project Director
- Division Chief (EES)
- School/Laboratory Director
- Dean/Director—EES
- Accounting Office
- Procurement Office
- Security Coordinator (OCA)
- Reports Coordinator (OCA)
- Library, Technical Reports Section
- Office of Computing Services
- Director, Physical Plant
- EES Information Office
- Project File (OCA)
- Project Code (GTRI)
- Other

CA-3 (3/76)

GEORGIA INSTITUTE OF TECHNOLOGY
OFFICE OF CONTRACT ADMINISTRATION

SPONSORED PROJECT TERMINATION

Date: 1/23/79

Project Title: Comparative Evaluation of Woven-Graphite Epoxy Composites.

Project No: E-16-604/E-27-654

Project Director: Dr. S. V. Hanagud/Dr. A. Tayebi

Sponsor: NASA-Langley Research Center

Effective Termination Date: 10/31/78

Clearance of Accounting Charges: 10/31/78

Grant/Contract Closeout Actions Remaining:

- _ Final Invoice and Closing Documents
- _ Final Fiscal Report
- x Final Report of Inventions
- x Govt. Property Inventory & Related Certificate
- _ Classified Material Certificate
- x Other SF Form 272 (Final)

Assigned to: Aerospace Enginering/Textile Engineering (School/Laboratory)

COPIES TO:

- Project Director
- Division Chief (EES)
- School/Laboratory Director
- Dean/Director—EES
- Accounting Office
- Procurement Office
- Security Coordinator (OCA)
- Reports Coordinator (OCA)
- Library, Technical Reports Section
- Office of Computing Services
- Director, Physical Plant
- EES Information Office
- Project File (OCA)
- Project Code (GTRI)
- Other_____

CA—4 (3/76)

Final Report
E-16-604

COMPARATIVE EVALUATION OF WOVEN GRAPHITE-EPOXY COMPOSITES

Principal Investigators: S. Hanagud (A.E.)
A. Tayebi (Textiles)

Research Assistants: R. G. Clinton
B. M. Nayak

ABSTRACT

A comparative evaluation of some of the mechanical properties of woven graphite-epoxy composites have been discussed in this report. In particular the types of weaves and the resin contents have been chosen for comparison. The types of weaves selected are plain weaves, satin weave and tri-directional weave. The composites made of these fabrics have been compared to composites made from unidirectional tapes under static and fatigue loading. During static loading acoustic emission events have been monitored. Also, examinations of fracture surface and polished sections of specimens away from the fracture surface under an electron microscope have been discussed.

TABLE OF CONTENTS

INTRODUCTION

The future high cost of energy and their limited availability resulted in the need for designing aircraft that can maintain the present levels of performance with a decrease in the level of fuel consumption. One way of fulfilling this need is by using materials that offer a high strength to weight ratio than are offered by the currently used aircraft structural materials. Advanced composites offer such a potential. Preliminary projections indicate[1] that as much as twenty percent reduction is possible in the design of airframe subassemblies by using graphite-epoxy composites. Such a reduction of weight in the airframe subassemblies can lead to a reduction of gross take off weight in the range of five to fifteen percent. Similarily, a development of advanced composites that are capable of operating at high temperatures might improve the thrust to weight ratio by as much as 25%.[2] Such an improvement leads to an additional reduction of takeoff gross weight by an amount larger than 10%.[2]

These potential benefits have resulted in an increased research activity among structures and materials engineers. Some of the research activities are concerned with the environmental effects, the techniques of decreasing the cost of production, the development of nondestructive inspection procedures, the techniques of life estimation, the development of fail-safe design procedures, the foreign object damage, the damage, the damage tolerance and the dynamic properties of composites. Most of the investigations in the field of graphite-epoxy composites have been conducted with uniaxially reinforced lamina or laminates. However, graphite epoxy composites can be produced by using single or multiple layers of woven graphite fabrics and epoxy. Very little work has been

reported in the field. Most of the reported work is concerned with the fabric and not composites.[2-8]. These woven graphite-epoxy composites offer a potential reduction in the cost of production of actual structures.[9] For example, the use of woven fabric concept in fabricating NASA telescope metering truss has resulted in a reduction in the cost of labor from two-man days to two hours. Other potential benefits of woven graphite-epoxy composites include a lower probability of delamination than in uniaxial reinforced composites. Inspite of these potential benefits there is very little research work reported in this field. Therefore, an investigation leading to the comparative evaluation of the woven graphite epoxy composites is being conducted by the authors. This report describes the results of the investigations.

PROBLEM SETTING

Woven fabric composites or woven composites consist primarily of woven fabrics and epoxy. Different woven fabric composites are characterized by the different type of weaves, different percentages of epoxy in the composite, different stacking sequence, different number of layers and different geometry. In this report, the evaluation of woven composites are restricted to different types of weaves and different percentage of resin content. In particular, plain weave, (Figure 1a) satin weave (Figure 1b) and tri-directional weave (Figure 2) have been considered whenever possible. The mechanical properties of these composites have been compared to those made from unidirectional tapes. Different resin content varying from 20 to 50% have been considered for purposes of evaluation of woven composites. Only tensile loading and fatigue loading have been considered. The mechanical properties to be evaluated and compared include the failure stress, the specific failure strength, stress-strain behavior and the acoustic emission behavior. In addition to

the investigation of these mechanical properties, the study also includes the analysis of the facture surface by using a scanning electron microscope. The Acoustic emission has not been considered for the case of fatigue loading.

SPECIMEN PREPARATION

Weaving

The first task of the project was to develop a capability to weave graphite fabrics from graphite yarns at Georgia Tech. In particular, the capilities for producing fabrics of plain weave, satin weave and tri-directional weave were sought. The plain weave fabrics and the satin weave fabrics were produced by using hand loom techniques (Figure 3). The choice of hand loom was because of the non-availability of a proper power loom that would assure prevention of damage to graphite yarn. Union Carbide's Thonell 300 that has 3000 fiber per yarn was used. The production started by winding the yarn off the commercial spool on to a single ended warper. This operation was done to produce evenly spaced yarns that were eventually wound on a warp beam for purposes of weaving. In the whole process, the major emphasis was on the protection of graphite fibers. A layer of paper was wound between the layers of graphite yarn to prevent the rubbing of yarns. Several glass rod guides were used to control the movement of warp yarn. All fabric had equal number of fiber in warp and fill directions. The looms were capable of producing fabrics of different ends per inch. The single end warper was also used to produce unidirectional tapes of desired number of ends per inch.

In order to compare with the plain and the satin weaves of twelve or more end per inch, a fabric of tri-directional weave of comparable ends per inch was needed. In order to achieve this objective, the School of Textile Engineering at Gerogia Institute of Technology bought a Gloor

Tri-weave machine. However, the investigators, had difficulties in adapting the machine for producing graphite fabrics of tri-directional weave. The principal reasons for the difficulty in adapting the machine for graphite yarns were the complicated yarn path and coarse eyelets. These difficulties were eliminated by designing a set of copper tubes for guiding yarn. It was also demonstrated that the use of copper tubes will eliminate the possibility of damage to graphite yarn. However, 188 such tubes needed to be installed for obtaining the desired ends per inch. It was not possible to install the desired number of tubes during the project. As an alternative, tri-directional frame weaving technique was used to produce the needed fabrics for the project. The details of the frame weaving technique are illustrated in the figures 4,5 and 6. The figure 3 illustrates the warp yarns at $+30^{\circ}$ and -30° and fill yarns at 90°. The only difficulty with frame weaving was that the finished fabric was restricted to 7 ends per inch. This restriction is imposed because of the maximum area of the overlapping triangle (See figures 2 and 4). The figure 5 shows the size of warp yarns required to produce a net size of 12"X12" fabric.

Fabrication

The process of production of both plain and satin weave panels was very nearly the same with minor exceptions. First, the fabric was cut into properly sized sheets, 9½" x 12" with 0° axis being in the warp direction. The sheets were weighed individually to obtain the total fiber weight and to determine the amount of resin needed. The solid epoxy resin was combined with acetone as solvent in a 50/50 mixture and stirred for a minimum of three hours as recommended by the manufacturer. Acetone was added periodically to maintain correct ratio. The sheets of fabric were then impregnated with the resin solution by pouring the solution

(amount equalling twice the weight of the fabric) over the fabric and then rolling with an aluminum roller to ensure penetration into the weave and fibers. The sheets were then set aside to allow the acetone to evaporate for twelve hours or more. At the end of this period, the sheets would ideally be a 50/50 ratio of fiber to resin with an allowances of 2% for roll-off and the excess acetone which did not evaporate.

The stacking sequence is shown in Figure 7 and will be briefly explained for each laminate. The area of the base plate containing the laminate was enclosed by a cork dam, and the surface within the dam was coated with a release agent. A layer of 1 mil. teflon was next put on the plate to eliminate bonding of laminate to plate. The graphite/epoxy fabric sheets were laid up outside the dam and then placed within after rolling with rubber roller to remove trapped air. The stacking sequence was the same for both panels with the warp direction being the 0^{o} axis or longer dimension. The laminate was sandwiched between layers of TX1040, a pourous teflon-coated release cloth again to prevent cobonding of laminate to plate or bleeder material. The bleeder material was placed directly above the TX1040. Generally, the rule for the amount of bleeder material is a layer of bleeder for every 3 layers of prepreg, The bleeder used was as follows: One layer of 181 glass and 3 layers of 120 glass. Since the 120 glass is 60% as absorbent as the 181, this yields a total of 2.8 sheets of 181 which is very close to the 3 to 1 rule. A similar arrangement was designed for satin weave.

Topping the bleeder material was another layer of teflon on to which was placed the perforated, release-agent coated top aluminum plate. This lay-up assembly was sealed by placing a commercial sealer strip between top plate and cork dam. Through the holes in the top plate,holes were punched in the teflon layer below to allow for excess bleeding. The

entire assembly was then placed in a vacuum bag composed of two sheets of 2 mil mylar and a sealer before connecting to a pump for 2 hours.

A slightly different stacking sequence was designed for tri-directionally woven composities. Such a sequence was designed by taking into account the limited quantity of available tri-directional fabric. These composites were made from four layers of tri-directional fabrics and three layers of satin fabrics. The layer of satin fabrics were used as the outer and the central layer.

For purposes of comparison, composites were made from uni-directional tapes. For example, to compare a woven composite consisting of 8 layers of plain weave fabric, a composite consisting of 16 layers of uni-directional tape and an appropriate stacking sequence was produced. Similarly tapes were laid at $+30^{\circ}$, -30° and 90° to produce composites for comparing with tri-directionally woven composites.

Different resin contents were obtained by controlling the initial amount of epoxy used, temperature of a drying cycle that was used prior to curing, the pressure and temperature of the final curing cycle. It is to be noted that the resin content of 50% was first obtained by accident. By analyzing the cause of the accident a better curing cycle and a better control of the resin content was obtained.

Curing

This phase consisted of stacking the lamina in prescribed sequence and then placing the laminate in an oven for about 2 hours at 100° C to evaporate the acetone. The prepreg staging has a great influence in controlling the quality of the laminate, as will be described, for the individual panels. The cure cycle is as follows:

1. Pre-cure for 2 hours at 100° C, allow to cool
2. Vacuum bag entire assembly
3. Apply full vacuum for 2 hours to debulk at room temperature
4. Maintain vacuum throughout entire cycle
5. Place in press and raise temperature to 250°F at 2°-5° F per minute under minimal pressure
6. Hold at 250 (+5°-10°F) for 15 ± 5 minutes, apply 100(+5-0 psi.)
7. Hold at 250 (+5°-10°F) and 100(+5- 0 psi.) for 45 ± 5 minutes
8. Increase the temperature to 350 (+10° -0°F) at 2° - 5° F per minute
9. Hold at 350 (+10, -0°F) for two hours ± 15 minutes
10. Cool under pressure and vacuum to below 175°F

For individual laminates the step (1) and the pressure in the final curing cycle varied.

Tensile Specimens

The panels were first trimmed one inch on all sides to prevent non-uniformities in thickness. The panels were then cut into specimens by use of an abrasive wheel. The final dimensions were obtained by grinding with a diamond wheel. Examination of the edges of all specimens showed no rough surfaces or notches. The dimensions of each specimen, in accordance with ASTM specifications: length = 10 inches, width = 1.006 inches, was maintained whenever possible.

Aluminum tabs measuring 1½ inches in length by 1/3" thickness and 1 inch wide with a 15° level were bonded to the specimens with Eastman 910 adhesive.

TESTS

All tensile tests under static loading were conducted in an Instron Universal Testing Machine. The speed of the cross head was set to provide a strain rate within the tolerances of A.S.T.M. specifications. Several

laminates were instrumented with strain gages for monitoring the stress-strain behavior. During most of the tests acoustic emission was monitored by using Dunegan-Endevco 3000 series equipment as shown in the figure 8. Two transducers were mounted on the outside of the specimen to serve as guard transducers for purposes of filtering the signals that have sources outside the gage length of interest. A central transducer was mounted to monitor the acoustic emission data. With the exception of tests 42-52, the guard transducers were Dunegan-Endevco S 140 B/HS and the data transducer was Dunegan-Endevco S 140 B. Because of the reduced gage lengths in tests 42 to 52, acoustic emission technology micro miniature transducer MC 500 were used as guard transducers and DE S140B/HS was used as data transducer.

A data acceptance region was established by both guard transducers and the data transducer. Events that occurred outside the region did strike the guard first. As a consequence, the data collection process was shut down and the unwanted signals such as the grip noise were eliminated. On the other hand, an event originating within the region of acceptance created a pulse that did strike the data transducer first and produced a signal which passed through a 40 db preamplifier, a band pass filter, an adjustable gain amplifier, a threshold counter and a distribution analyzer. Accepted cumulative events and counts were plotted on an x-y plotter.

The tensile fatigue tests were conducted in an M.T.S. system. The specimens, used for fatigue tests, had a central hole of ¼ inch diameter. The specimens, from the same batch with an identical central circular hole, had been tested in an Instron Testing Machine to obtain static ultimate strength. The specimens were tested at a mean load of 80% of this ultimate strength. An oscillating load of $\pm$ 10% of the ultimate load was selected. All specimens

were tested at 30 cycle per second.

After completion of the testing program, the fracture surface of one specimen of each type of laminate was examined by using a scanning electron microscope ISI-60. The fracture surfaces were mounted on aluminum stubs and coated with gold before examination. Similar examinations were conducted on (a) sections from fractured laminates taken away from the fracture surface and (b) sections from unfractured laminates for purposes of comparison. These sections were first mounted in epoxy and then polished. The polished specimens were later coated with gold for S.E.M. examination. The useful magnifications varied from 50X to 30,000X. Selected areas were photographed.

RESULTS AND DISCUSSION

State Test

The Table I shows the results of all recorded tests. The test numbers are not in sequence. This is necessary to group the type of weave and resin content. The table displays the percentage of resin content, the type of weave, lay-up, thickness, gage length, ultimate load the total detected acoustic emission events and the total detected acoustic emission counts under a fixed threshold of one volt after the selected amplification and filtering operations. A double asterisk is used to indicate specimen with holes.

The Table II illustrates the group mean values of ultimate stress in psi and the standard deviation. Similarly Table III illustrates the group mean values and standard deviation for ultimate stresses for specimen with circular holes. The values of standard deviation from Table II indicates an appreciably lower scatter in woven composites when compared with the unidirectional composites. When plain weave and satin weave are compared the plain weave specimen offer a lower scatter. The tri-directional weave has the lowest scatter in the observed results.

As expected, the ultimate stresses for plain woven composites are lower than that of uni-directional composites. In some cases, the satin weave with larger end per inch but same total weight of fiber, has the highest ultimate stress of tested specimens. This weave offers the advantages of fabrication that are characteristic of woven composites while retaining the strength. The reduction in strength of plain weave almost disappeared when a stress concentration in the form of hole is persent. However, in the conducted tests, satin weave displayed a lower strength in the presence of a hole when compared with unidirectional specimen of the same resin content. However, the number of samples tested were small to draw any specific conclusions.

The Table IV illustrates a comparison of specific strengths with the type of weave and the resin content. The specific strength is defined as the ratio of strength in psi to the density in pounds per cubic inches. The table is arranged in decreasing order of specific strength. All results in this table are for specimens without stress concentration. Under tensile loading, 30.2% satin weave offers the best specific strength or strength to weight ratio of the tested specimens. These specimens, however, had higher ends per inch. The 30% plain weave has only a reduction 6% specific strength when compared to unidirectional weave. The two ultimate strengths are much closer to one another when holes are present. The tri-directional weave displays the lowest strength of all weave with resin content in the range of 30-37%. The reason for the low values are due to the low ends per inch and voids. Table V and VI illustrates the comparison of modified ultimate stress. This comparison was done in addition to the specific strength for the following reasons. In calculating specific strength, the value of density was needed. These densities were calculated for a given panel. However, the thick-

nesses were measured accurately for each specimen. Then the two ultimate strength can be compared by assigning a weight based on the density ratio. The modified ultimate stress is then derived as follows:

$$mu = \frac{u\ t_G}{t_{G\ min}}$$

In the equation, t_G is average group thickness and t_{Gmin} is the lower of two t_G values. It is to be noted that the width of each specimen was the same. The total number of fiber in each panel was the same. Then for the same total number of fiber, same width and length, the thickness of the woven composite is usually more. The resin content being the same the thickness controls the strength to weight ratio. On this basis, the reduction in specific strength is of the order of 3-6% for specimens without holes. For specimens with holes, woven specimen have higher strength. However, it is to be noted that number of tests with holes were small.

Acoustic Emission

The figure 8 illustrates the plot of acoustic emission events versus time for composites containing 37% resin content and made of plain weave fabric. The cross head speed for these tests were 0.1 inch minute. The results of tests 15, 16 and 17 display almost identical results during the first half of the test duration. The number of events differ only by about 10% during the next fifteen seconds for these tests. Later, the plots separate as failure approaches. These specimens with nearly identical plots also had failure load within 5% of each other. The failure loads were 5700, 5750 and 5500 pounds. The specimen 10, however, displayed increased early emission activity. The emission rate increases faster than that for the group 15, 16, and 17. The increase of acoustic emission activity suggests the possibility of pre-existing damage or a substandard specimen. This hypothesis is supported by the lowest failure load of 4200 lbs for this group. The

specimens 15, 16 and 17 had an average failure load of 5650 pounds. The acoustic emission event pattern for specimen 10 shows an increased early emission activity somewhere between the "standard pattern" of the specimens 15, 16 and 17 and an extreme pattern of the specimen 10. However, for a short time, the pattern appears to return to the standard pattern only to display an increased emission rate during the middle of the test. The increased early emission activity and an increased emission rate during the middle of test suggests the possibility of damage or substandard specimen. Also all the activity lies between the standard pattern and the extreme of test 10. The quality of the specimen can be expected to lie between the standard and the extreme of the specimen 10. This hypothesis is again confirmed by the failure load of 5100 pounds which is between the average of 5650 pounds and the lowest value of 4200 pounds for the specimen 10.

The figure 9 illustrates the plot of acoustic emission events versus time for a composite made of plain weave containing 22% resin. This is the only specimen of this type for which the acoustic emission has been monitored. The results will be compared with the specimens of plain weave and 37% resin. This plot follows the pattern of the test number 10 rather than the "standard" of figure 8. The ultimate load again is 4050 pounds which is quite close to that of specimen 10 which is 4100 pounds. The resin content of 22% rather than 37% can be considered as the substandard quality of the specimen. Thus, these two figures indicate that the early emission activity compared to a standard and the increase activity during the middle of the test is an indication of the quality of the specimen.

The figure 10 shows the plot of acoustic emission events versus time for three composites containing 50% resin and plain weave fabric. The cross head speed is again 0.1 inch per minute. The specimens 12 and 13 initially follow

the "standard emission pattern" of specimens 15, 16, and 17 are illustrated in figure 8. However, the emission rate increases during the middle of the test. The increased rate lies some where between that of the standard pattern and the extreme of test number 10. The failure load for these specimens has a mean of 4650 pounds. This value is higher than the extreme case of the test 10 and lower than the considered standard of tests 15, 16, and 17. The acoustic emission pattern of the test 4 is different. It shows an increased emission rate during the middle of the test. This activity decreases later. The specimen had an ultimate load of 5000 pounds. The sudden switch in the emission rate also coincides with higher ultimate load. The key points useful in comparison appears to be the departure from the standard acoustic emission events and the standard emission rate.

The figure 11 shows the variation of acoustic emission events versus time for tri-directional weave. It is to be noted that the fabric used in this case had only seven ends per inch. Because of the open weave large spaces for matrix concentration and voids is available. The tests were conducted at a cross head speed of 0.05 inch per minute. The resulting acoustic emission plots are well grouped. All specimen are of the same quality. The specimen 50 which has the highest rate of emission during the early part of the test had the lowest failure load in the group. The specimen 49 which had the lowest emission rate during the early part of the test had the highest failure load in the group. As a group, the emission can be compared to the plain weave composites containing 37% resin content (figure 8). After appropriate corrections for the cross head speed the average emission rate for tridirectional specimen is approximately half that observed for the "standard pattern" of the specimen 15, 16, and 17 of figure 8. It is also to be noted that the average failure load for the tri-directional specimens

is 2950 pounds and the average failure loads for specimens 15, 16, and 17 is 5650 pounds.

The figure 12 shows the acoustic emission events variation for composite specimen prepared from unidirectional graphite tapes and containing 37% resin. These plots display considerable scatter just like the scatter in the failure loads displayed in the Table I. The cross head speed for these tests are 0.1 inch per minute. The figure 13 shows the acoustic emission results for a composite made from unidirectional tape and containing 50% resin. The results of this series of tests are best analyzed by beginning at the Fabrication Stage. As mentioned earlier, this panel is precured before the final cure cycle began. A higher precuring temperature than normal is responsible for high resin content. Therefore, many air bubbles are trapped causing visible voids. This high void content greatly reduced the strength of the specimens. The acoustic emission event graphs of figure 12 show that specimen 14 has early activity over a short followed by gradual increase in slope, while specimens 5 and 18 do not show activity until much later time. The patterns of specimens 5 and 18 can be seen to be nearly identical with the exception of the sharply increased activity of specimen 18 before failure which is not uncommon. Discounting the initial spurt of events in test 14, this path coincides closely with the other two with exception that the rate of increase of the slope is higher as failure approaches. All specimens show a mark increase in event rate shortly before failure. The failure loads reflect the emission rates; the loads are not identical but grouped reasonably well. The fact these are less acoustic emission events in a poor quality specimen is suprising.

The figure 14 show the acoustic emission events for specimen with holes. The tests 21 and 22 are for composites of plain weave with 37% resin and ¼ with diameter hole. The specimen 23 is a composite from plain weave fabric

and 50% resin. The specimen 24 is a composite prepared from unidirectional tapes and 37% resin with a hole of ¼" diameter. The number tests of particular type are too few to provide any comparison.

Fractography

Fracture surfaces of various laminates are examined under the scanning electron microscope, model ISI-60. This examination is not intended to qualify the specimens but to study the surfaces and determine if any additional information can be obtained from this method of inspection. Several interesting features are observed; some pertaining to possible explanation of failure and others on fiber surface pattern differences. Figures 15, 16, 17 and 18 are the magnified pictures of fracture surface of a composite from plain weave fabric and containing 22% resin. Similar observation have been made on facture surface of plain weave fabric and 37 to 37% resin. This particular specimen has a failure load of 4050 pounds much less than the average load for good quality specimen which is 5650 pounds. The S.E.M. examination is conducted to explain the reaspms for the low failure load.

The figures 15 and 16 show the voids. In particular, the figure 16 shows the oval shaped smoothly contoured areas. The figure 15 shows areas where these were pre-existing fiber breaks before the composite was produced. The figure 17 shows the origin of delamination. The figure 18 is the magnified image of a portion of the fracture surface at 12K. A single fiber can be observed. This figure shows the normal tension failure of a single fiber. A smooth area at the crack origin followed by radial lines, can be observed. It is to be noted that there is a small hole at the crack origin. This is hypotherized to be a pre-existing flaw in the fiber where the tension failure originated.

The figures 19, 20 and 21 is for a composite of 50% resin and plain

weave. This shows a type of propagation of cracks through the fiber bundle. The crack origin is at the junction of two fibers. A change in the direction of propagation at the upper left fiber and the right fiber can be seen. However, at the junction of the lower left fiber and the right fiber, the crack propagates without change of direction.

The figure 20 shows the damage incurred before curing to a complete bundle of fibers. Near the upper edge, many little bumps are seen. These are actually bundle of broken fibers which have been coated with matrix in the curing process. The decrease in strength locally would be severe. The figure 21 shows several partially damaged bundles. The damaged regions do not appear clean and sharp, instead the fibers look as they have been washed down. Also the delamination arrested by the weave pattern in upper left corner around the 0^{o} fiber and following the transverse fiber can be seen in this figure.

The figures 22 and 23 are from a plain weave specimen which showed very poor failure load. The reason for this can be observed in the pictures. The specimen shows extreme fabrication damage. In figure 22 and 23 well over half of the available 0^{o} bundles were broken and covered with matrix. Theve are the bumps on the surface. The figure 24 shows how the cross-section should normally look like. The figure 24a is for 37% plain weave shown for comparison. The fracture surface is smooth no large pull-outs. This specimen of figure 24a had one of the very high failure loads.

The figure 25 is a magnified picture of a polished section of a composite specimen of plain weave fabric and 37% resin. The section is at a short distance away from the fracture surface. No unusual fracture pattern is observed. In fact the figure 25 is very similar to the figure 26 which is the magnified picture of polished specimen of an unfractured or virgin specimen. The figures 25 and 26 are at ap-

proximately 5K magnification. The figure 27 is a lower magnification picture of a section from a virgin specimen. The fiber bundles, as they appear in woven composite, can be seen. The figure 28, however, is from a section of failed composite very close to the fracture surface. This picture is from a polished section at a magnification of 9.8K . Some cracks at the fiber-matrix interfaces can be seen. A large number of fibers and matrix can be seen at 1K as shown in the figure 29. This figure can be compared to the figure 30 which shows no such cracks. The figure 30 is, however, from a section of a virgin specimen. In the next few figures, the plain weave fracture surface have been compared to the fracture surface from composites made from unidirectional tapes. The figure 31 shows the view of a cure section with double 0^{o} layer at the center and 90^{o} ply on the outside. This picture can be compared to the figures 16 and 17 of plain weave. The clean appearance of 90^{o} plies can be seen. Also no arrest of any delamination can be seen. The figures 32 and 33 show fractured single fiber. Pre-existing flaws can again be seen at the crack origin in both pictures.

The figures 34 to 36 show the magnified pictures of fracture surface from composites made from tri-directional weave fabrics. The resin content of 31% is present in these specimens. In figure 34. the difference between the central satin layer and the other tri-directional fabrics can be seen. The figures 35 and 36 show unusual fracture patterns that could not be explained. The figure 36, however, shows typical tension failure of fiber observed in other types of composites.

Fatigue Failure

Only five specimens are tested in tension fatigue. The number of specimens and their loading sequence is not sufficient for discussing any quantitative data or failure loads. However, the specimens are

mainly used to study the fracture patterns under a scanning electron microscope. All fatigue specimens are from composites from plain or satin weave fabrics. The resin content varied from 31 to 37 percent by weight. All the specimen had a central hole.

The inspection under S.E.M. is restricted to the area near the fatigue crack origin which was near the hole. The figures 37 to 39 show the fracture pattern of single fiber under magnifications varying from 7K to 11K. The fracture pattern of these fiber are very distinct from the fracture pattern of the fiber under static tensile loading as can be seen in figures 18 and 19. The fracture of these fiber are characterized by a smooth area over substantial part of the fiber. Also no stress concentration such as hole is seen at the crack origin. They appear to be cracks originated by fatigue. However, more tests are needed to confirm the hypothesis. Away from the crack origin standard tensile fracture pattern was observed. The figure 40 shows a number of such unusual fracture pattern. Similar observation on plain weave composites can be seen in figure 41 to 44.

CONCLUSIONS AND RECOMMENDATIONS

The woven fabric composites display specific strengths only slightly below that of composites made from unidirectional composites. This fact combined with a low scatter in the results and a potential for saving labor cost in fabrication makes the woven composites quite an attractive candidate material for aircraft structures. The satin weave combines the advantages offered by the woven composites and high strengths of unidirectional composites. However, plain weave specimens have practically no delamination displayed on the fracture surface. The tri-directional weave, even though contained only 7 ends per inch, displayed com-

parable strength. A closer weave can make this a very attractive candidate material. Non-destructive inspection procedures for quality control, estimation of ultimate load and flaw detection procedures can be established by using acoustic emission and emission rate. However, additional investigation, including quantitative models, are necessary.

A preliminary observation indicates that woven composites may be superior to unidirectional composites in fatigue behavior. Further work is necessary. Observation under scanning electron microscope provides tools for failure analysis and quality control. The quality control can be done by testing fractured and unfractured sample specimens from each batch of production.

REFERENCES

1. _____, "Work Shop on the Effects of Relative Humidity and Elevated Temperature on Composites," Sponsored by AFOSR, Newark, Delaware, March, 1976.

2. Ko, W. L., "Fracture Behavior of a Nonlinear Woven Fabric Material," J. of Composite Materials, Vol. 9, p. 361, 1975.

3. J. Skelton, "Strength of Textile Structures at High Strain Rates," J. Materials, Vol. 6 (1971), p. 634.

4. D. Roylance, "Ballistic Impact of Textile Structures," Text. Res. J., Vol. 43 (1972), p. 34.

5. W. C. Sleeman and T. G. Gainer, "Status of Research on Parawing Lifting Decelerators," J. Aircraft, Vol. 6 (1969), p. 405.

6. N. J. Abbott and J. Skelton, "Crack Propagation in Woven Fabrics," J. Coated Fibrous Materials, Vol. 1 (1972), p. 234.

7. W. D. Freeston and W. D. Claus, "Crack Propagation in Woven Fabrics," J. App. Phys., Vol. 44 (1973), p. 3130.

8. A. D. Topping, "The Critical Slit Length of Pressurized Coated Fabric Cylinders", J. Coated Fabrics, Vol. 3 (1973), p. 96.

9. _____, "Aviation Week, McGraw-Hill, New York, Jan. 26, 1976.

TABLE I

Test	Resin Content (%)	Material Layup	Thickness (in)	Total Counts (A.E.)	Total Events (A.E.)	Gage Length (in)	Ult. Load (
3	37	PW (12x12) 8ply	.063	511276	13843	7	5100
7	37	PW (12x12) 8ply	.065	NA	NA	7	4900
10*	37	PW (12x12) 8ply	.061	191290	17320	7	4200
15	37	PW (12x12) 8ply	.068	916076	30466	7	5700
16	37	PW (12x12) 8ply	.059	500,000	18,651	7	5750
17	34.4	PW (12x12) 8ply	.060	565676	25738	7	5500
21**	37	PW (12x12) 8ply	.067	13218	1461	7	2650
22**	35	PW (12x12) 8ply	.0615	31986	3025	7	2550
5	37	UD^{+}(90.0.90.0.90.0.90.0)s	.060	178391	44415	7	6700
9*	37	UD^{+}(90.0.90.0.90.0.90.0)s	.057	264929	20447	7	5300
11*	37	UD^{+}(90.0.90.0.90.0.90.0)s	.0575	104179	4978	7	4000
24**	37	UD^{+}(90.0.90.0.90.0.90.0)s	.056	19909	1551	7	2300
25	37	UD^{+}(90.0.90.0.90.0.90.0)s	.057	41126	2679	7	4570
	50	PW (12x12) 8ply	.0875	158556	10231	7	5000
2*	50	PW (12x12) 8ply	.085	376391	14743	7	4750
3*	50	PW (12x12) 8ply	.085	259081	14499	7	4550
3**	50	PW (12x12) 8ply	.085	10567	1099	7	2350
	50	UD^{+}(90.0.90.0.90.0.90.0)s	.088	43249	1540	7	3900
4	50	UD^{+}(90.0.90.0.90.0.90.0)s	.089	66100	2003	7	3500
8	50	UD^{+}(90.0.90.0.90.0.90.0)s	.090	20755	649	7	3370
7**	50	UD^{+}(90.0.90.0.90.0.90.0)s	.092	NA	NA	7	2175
8	31	Satin (12½x12½) 8ply	.060	NA	NA	7	5000
0**	31	Satin (12½x12½) 8ply	.060	NA	NA	7	2580
	18	PW (12x12) 8ply	.053	3174	159	6	3400
	18	PW (12x12) 8ply	.051	66720	1992	6	3800
	22	PW (12x12) 8ply	.055	1000000	33613	7	4050
0**	22	PW (12x12) 8ply	.052	91989	5799	7	2000
6**	30	UD^{+}(90.0.90.0.90.0.90.0)s	.048	NA	NA	7	1975

2*	30.4	PW (12x12) 8ply	.058	280100	Not Recorded	7	4725
3*	30.4	PW (12x12) 8ply	.0585	305659	Not Recorded	7	5250
4	30.4	PW (12x12) 8ply	.059	428474	Not Recorded	7	5500
5	30.4	PW (12x12) 8ply	.059	369229	Not Recorded	7	5400
6	30.4	PW (12x12) 8ply	.059	228196	Not Recorded	7	4450
7*	30.2	Satin (24x23) 4ply	.055	117441	Not Recorded	7	5550
8*	30.2	Satin (24x23) 4ply	.056	119799	Not Recorded	7	4900
9	30.2	Satin (24x23) 4ply	.0535	126746	Not Recorded	7	5600
0	30.2	Satin (24x23) 4ply	.055	101842	Not Recorded	7	5200
1	30.2	Satin (24x23) 4ply	.051	132907	Not Recorded	7	5100
2	30.3	5.-30.90.30.5.30.90.-30.5	.058	556525	21308	4	5400
7	30.3	5.-30.90.30.5.30.90.-30.5	.0575	152707	6615	4	4225
4	30.3	5.-30.90.30.5.30.90.-30.5	.059	510549	22426	4	5180
	30.3	5.-30.90.30.5.30.90.-30.5	.057	567361	21790	4	5180
6	30.3	5.-30.90.30.5.30.90.-30.5	.058	191975	11895	4	4780
3**	30.3	5.-30.90.30.5.30.90.-30.5	.056	46988	2392	4	2430
8**	30.3	5.-30.90.30.5.30.90.-30.5	.058	39543	1504	4	2300
9	31.7	Tri-Directional[1]	.064	814386	23753	4.125	3200
0	31.7	Tri-Directional[1]	.064	327140	8396	4.125	2600
1	31.7	Tri-Directional[1]	.063	414849	11748	4.125	2730
2	31.7	Tri-Directional[1]	.063	805528	21783	4.125	3190
9	31.7	Tri-Directional[1]	.063	NA	NA		3050
1**	31.7	Tri-Directional[1]	.063	NA	NA		2000

- Strain Data Available

*- ¼" Dia. Hole @ Center

- 12 Ends/Inch

PW- Plain Weave Fabric

UD- Unidirectional Pregreg Tape 12 ends/inch

Note 1: The tri-directional specimens layering configuration is satin/$3D_2$/Satin/$3D_2$/Satin where the 3D layers are woven graphite yarn with 6 ends/inch oriented -30/90/30 to the tensile axis. The 30.3% resin specimens were produced to compare with this laminate also using the 24x23 satin weave; designated satin Table I tests 42-48.

TABLE II

Group Values For Specimens Without Holes

Resin Content (%)	Material Configuration	Ultimate Stress (Psi)	Standard Deviation	σ_u (Psi) for Fiber unloading direction only
37	Plain Weave	83022	10460	166044
37	Unidirectional	94941	15836	189882
50	Plain Weave	55518	1834	111036
50	Unidirectional	40362	3552	80724
18	Plain Weave	69330	7324	138660
22	Plain Weave	73636	0	147272
30.4	Plain Weave	86275	7561	172550
30.2	Satin Weave	97525	6671	195050
30.3	Satin/Unidirectional	85533	7843	171066
31.7	Tri-directional	46601	4401	93202
31	Satin Weave	83333	0	166666

TABLE III

Group Values For Specimens With Holes

37	Plain Weave	40507	1351	74.36
37	Unidirectional	41071	0	72.01
50	Plain Weave	27647	0	53.05
50	Unidirectional	23641	0	47.18
22	Plain Weave	38461	0	79.05
30.3	Satin/Unidirectional	41524	2642	74.30
31.7	Tri-directional	31746	0	61.40
31	Satin Weave	31000	0	59.81
30	Unidirectional	41145	0	74.53

TABLE IV

Comparison of Specific Strengths

Specimen Type	Specific Strength (10^4 in)
30.2% Satin Weave (24 x 23)	176.46
37% Unidirectional Tape	170.11
31% Satin Weave (12 x 12)	159.74
30.4% Plain Weave	158.76
22% Plain Weave	158.20
30.3% Tridirectional Simulation	153.99
37% Plain Weave	147.88
18% Plain Weave	141.07
50% Plain Weave	106.85
31.7% Tridirectional Weave	90.31
50% Unidirectional Tape	77.42

TABLE V

Comparison of Group Modified Ultimate Stress

Specimen Type	Modified* Ultimate Stress
37% Plain Weave	90060
37% Unidirectional	94941

Specimen Type	Modified* Ultimate Stress
50% Plain Weave	55518
50% Unidirectional Tape	41867

Specimen Type	Modified+ Ultimate Stress
30.4% Plain Weave	89402
30.2% Satin Weave	97525

Specimen Type	Modified+ Ultimate Stress
31.7% Tridirectional Weave	51027
30.3% Tridirectional Simulation	85533

* Modified Ultimate Stress Defined to be: $\frac{t_{G(\sigma_u)}}{t_{min}}$ t_G represents group average thickness

+ Modified Ultimate Stress Defined to be: $\frac{\rho_{G(\sigma_u)}}{\rho_{sat}}$ t_{min} Lower of two t_G values
Where ρ_G is Density of Either Group

TABLE VI

Comparison of Group Modified Ultimate Stress

Specimens With Holes

Specimen Type	Modified* Ultimate Stress
37% Plain Weave	46474
37% Unidirectional Tape	41071

Specimen Type	Modified* Ultimate Stress
50% Plain Weave	27647
50% Unidirectional Tape	25587

Specimen Type	Modified* Ultimate Stress
37.7% Tridirectional Weave	35087
30.3% Tridirectional Simulation	41524

* Modified Ultimate Stress Defined to be: $\frac{t_{G(\bar{\sigma}_u)}}{t_{min}}$

Where t_G is the Group Average Thickness

And t_{min} is the Lower of the Two t_G Values

FIGURES

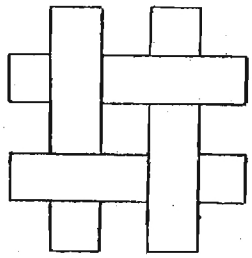

Fig. 1a Plain weave fabric

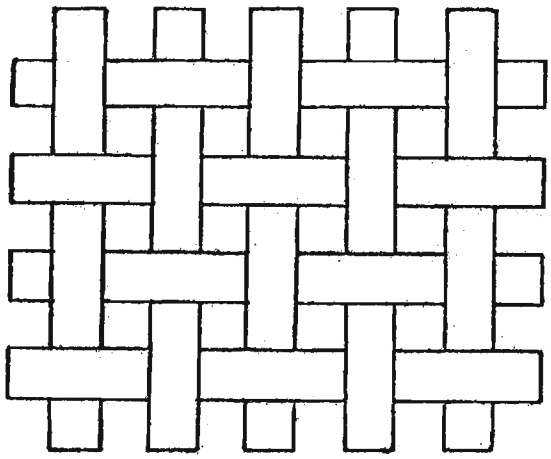

Fig. 1b Satin weave fabric

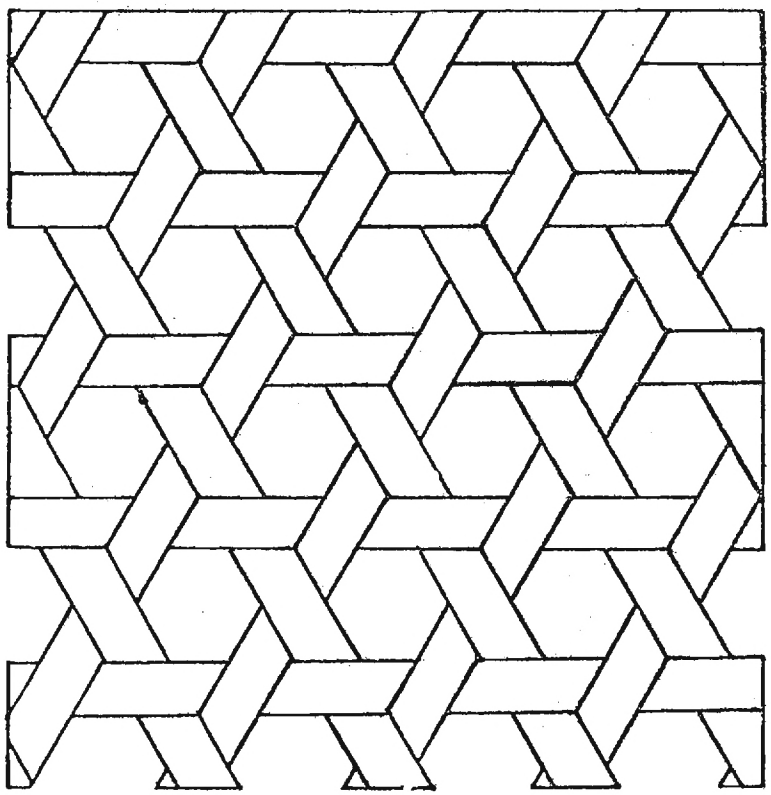

Fig. 2 Tri-directional fabric

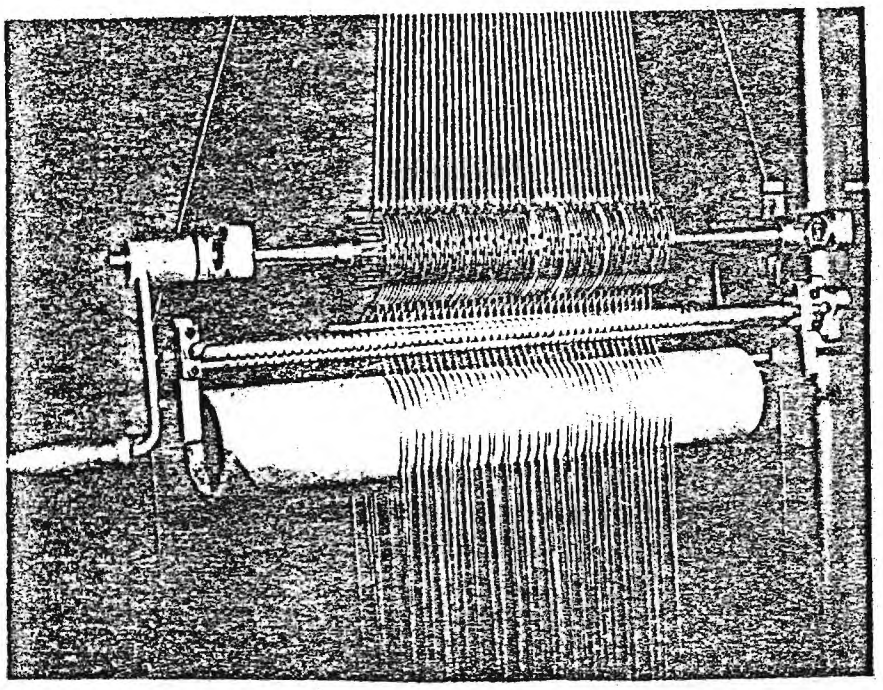

Fig. 3 Hand loom

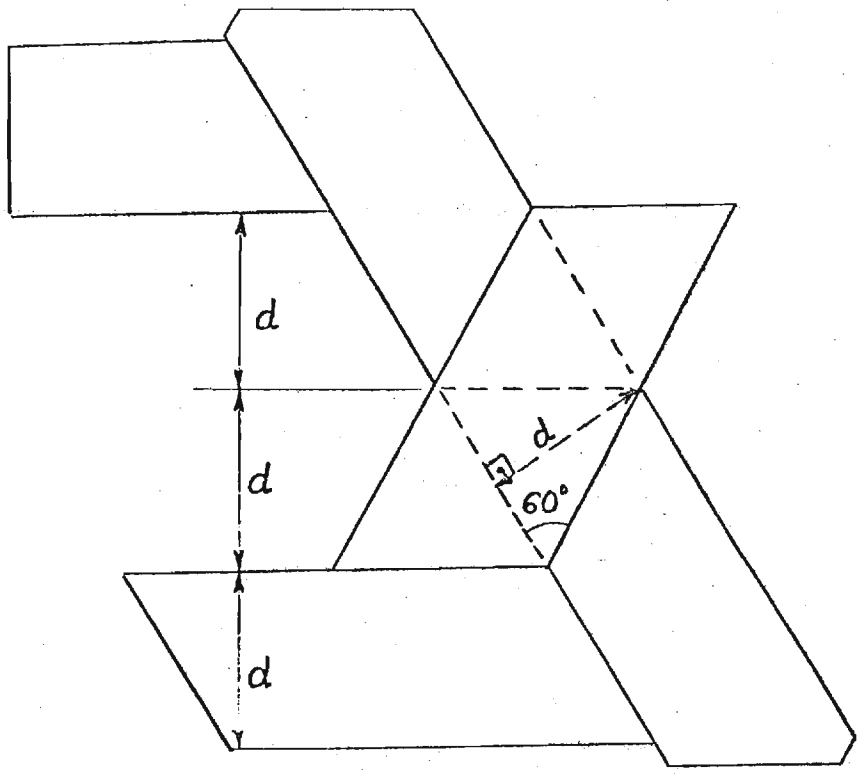

Fig. 4 Tri-directional weave - spacing

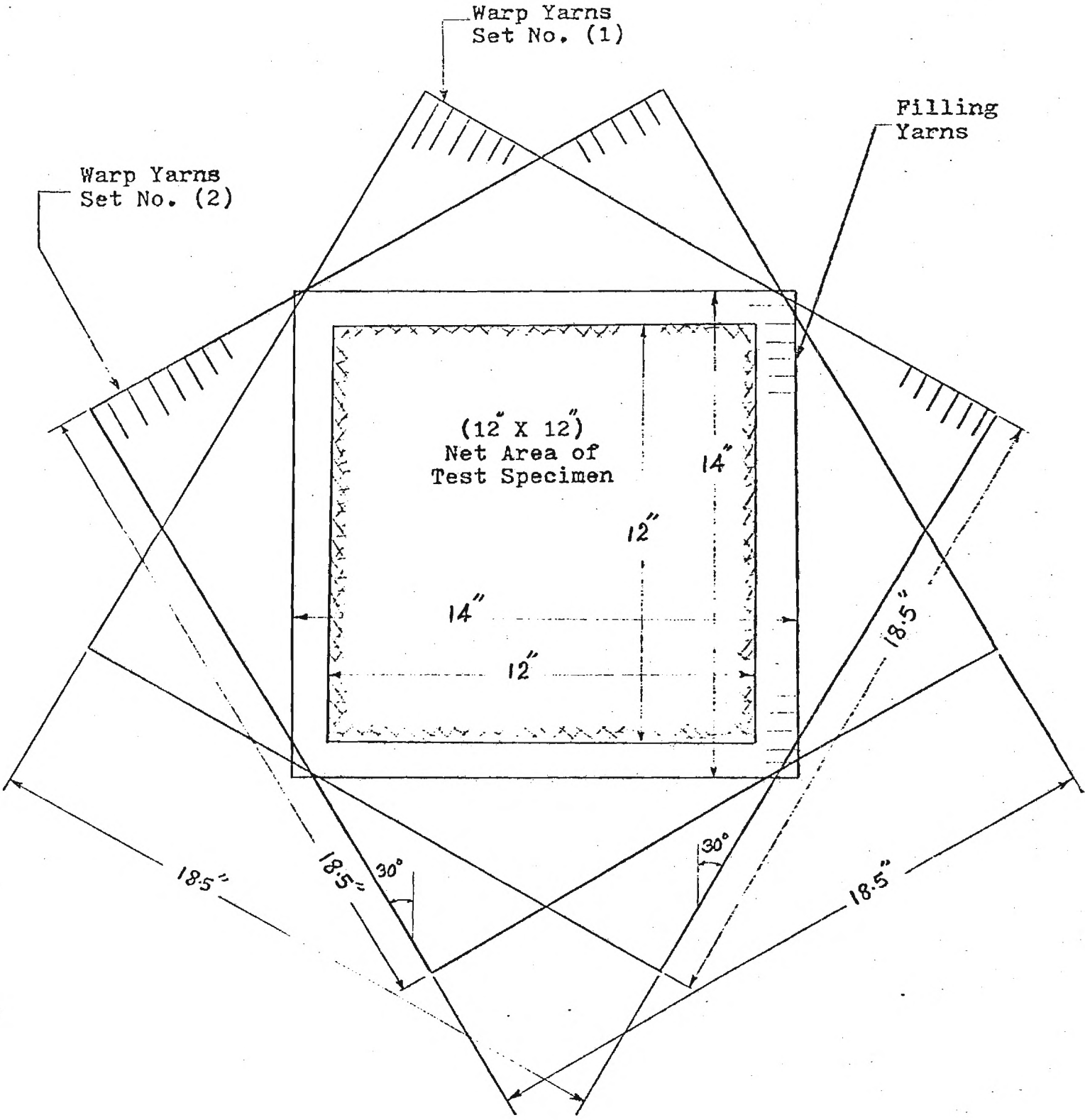

Fig. 5 Frame weaving of Tri-directional fabric

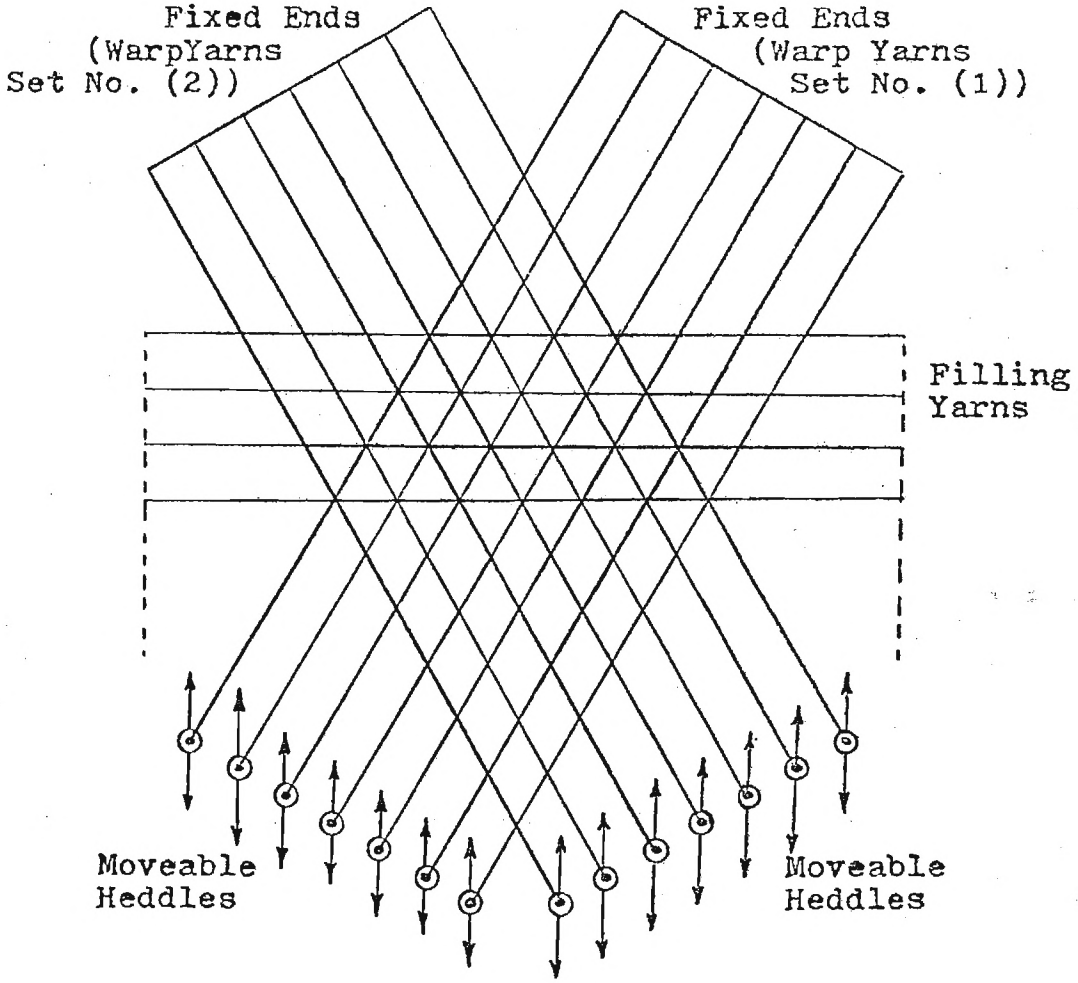

Fig. 6 Frame weaving of tri-directional fabric

Temperature - 340° - 350°

Pressure - 100 psi

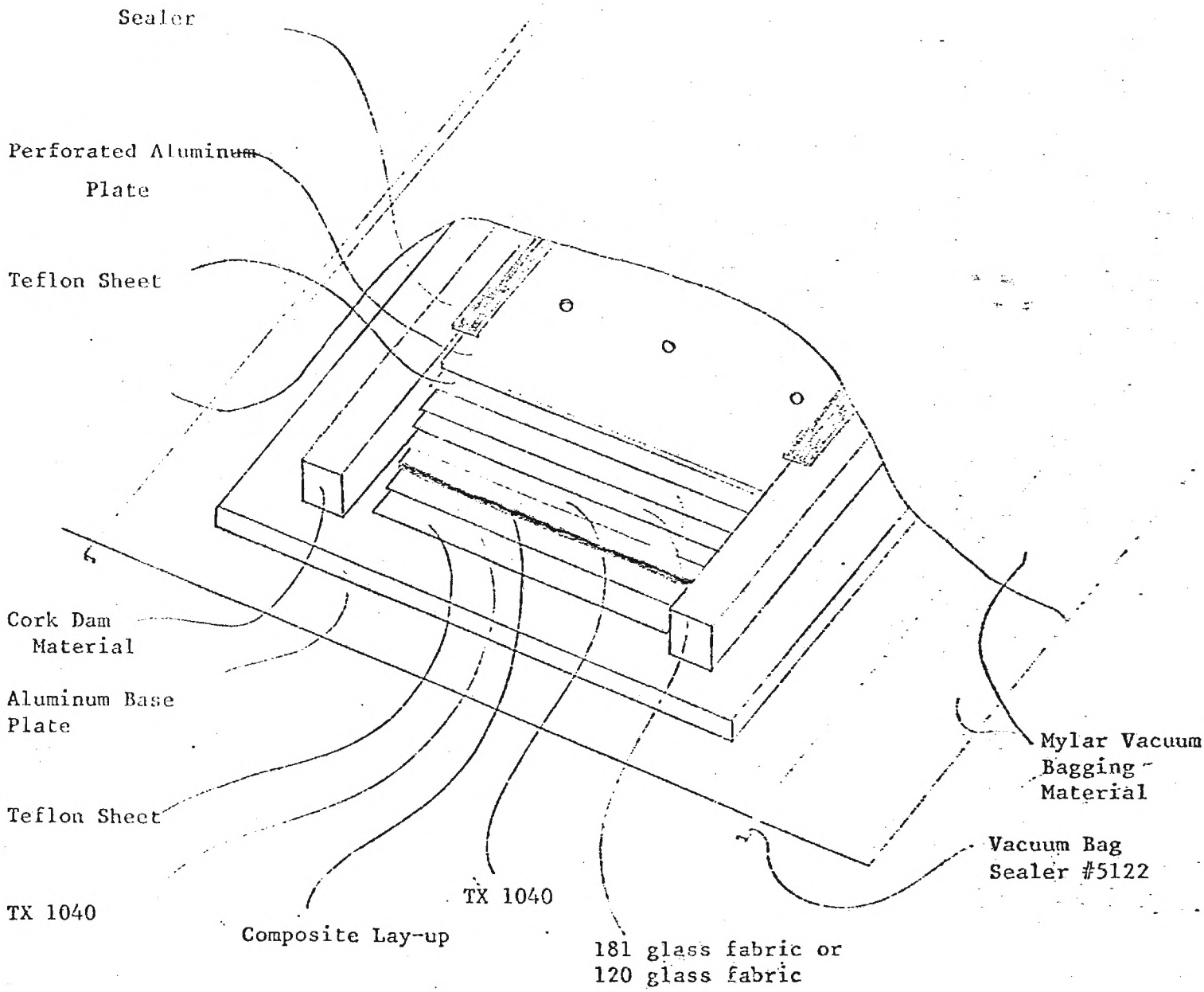

Fig. 7 Layering sequence

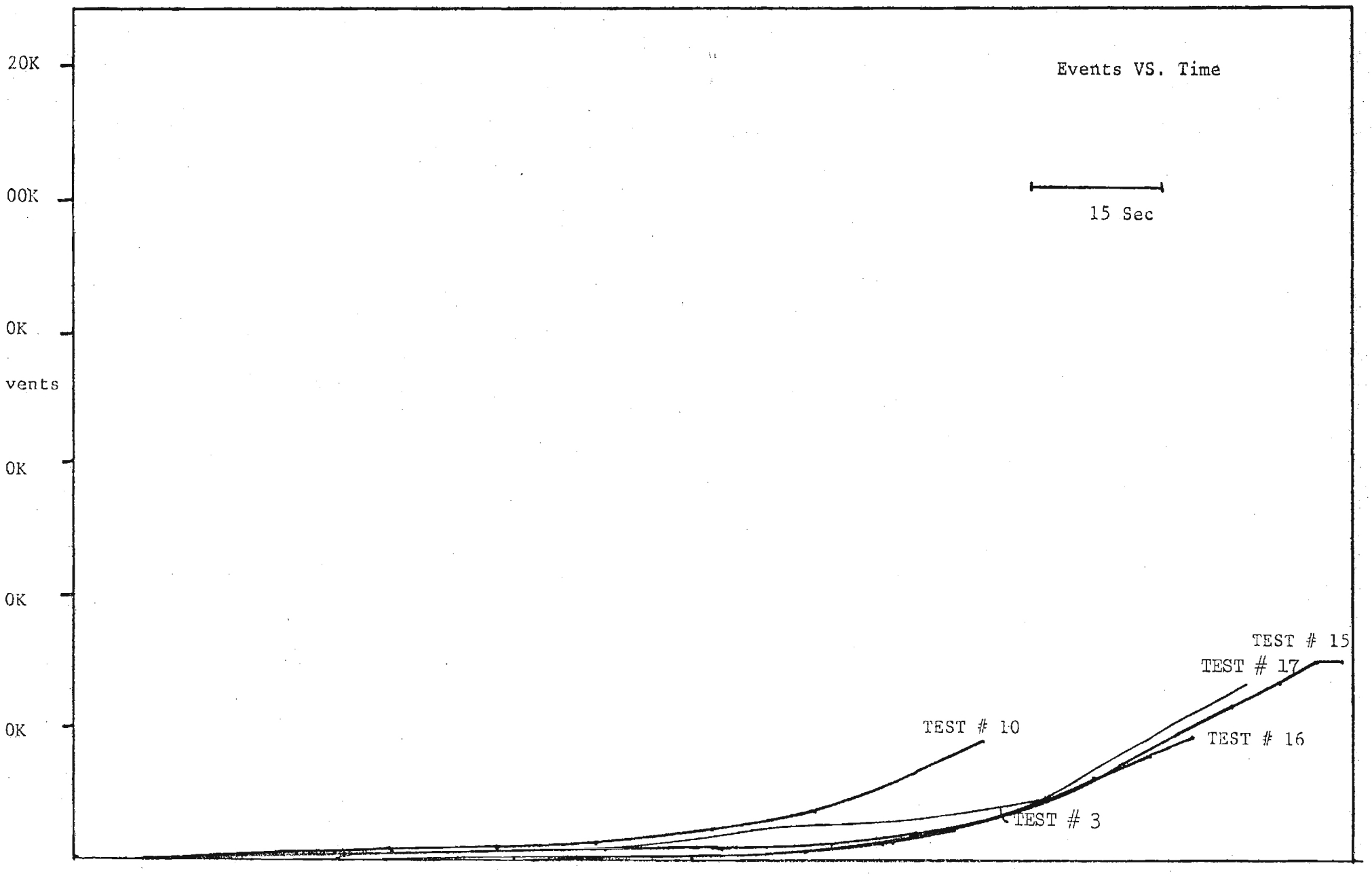

Fig. 8 Acoustic Emission events for 37% plain weave composite

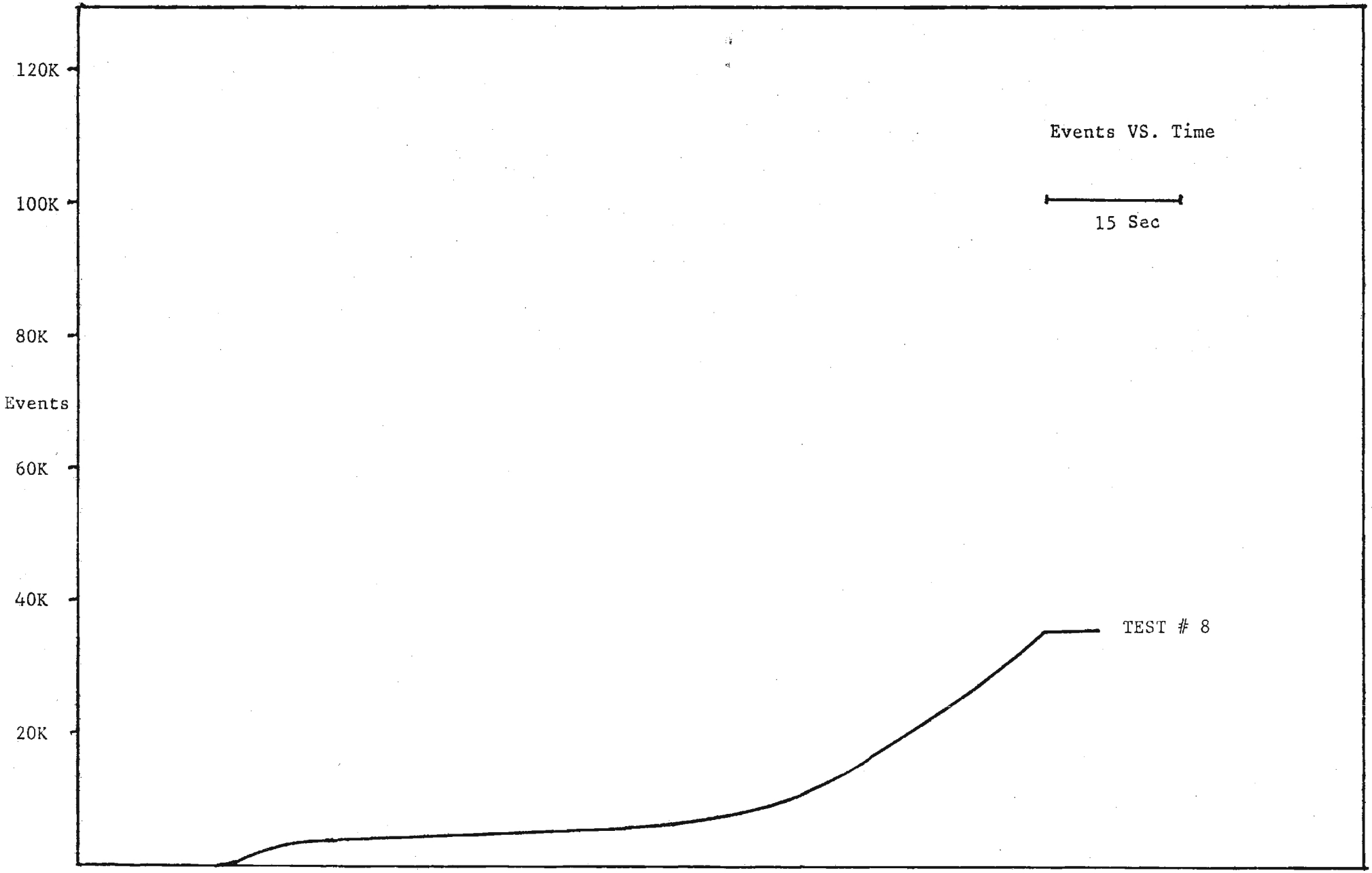

Fig. 9 Acoustic emission events for 22% plain weave composite

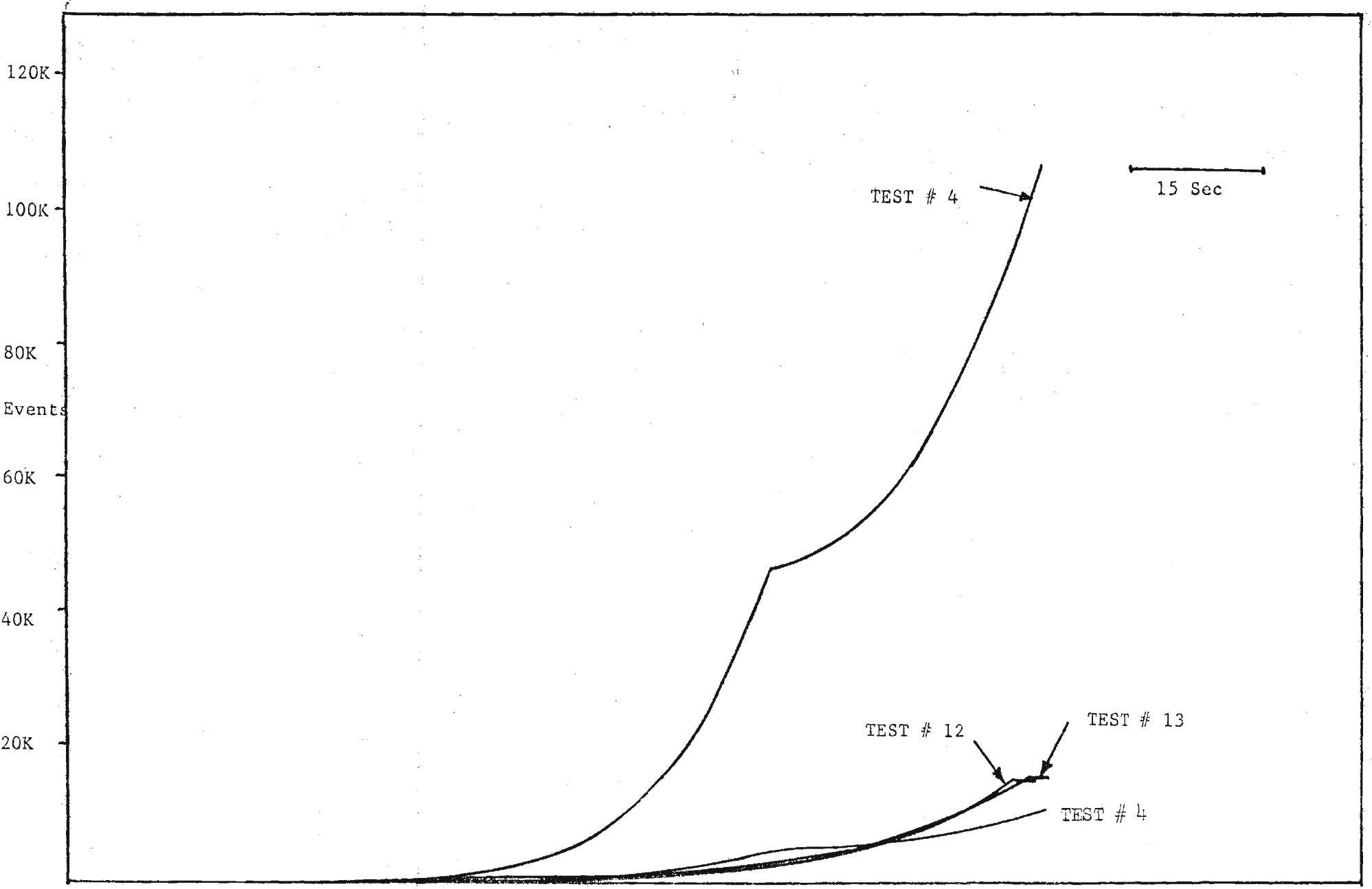

Fig. 10 Acoustic emission events for 50% plain weave composite

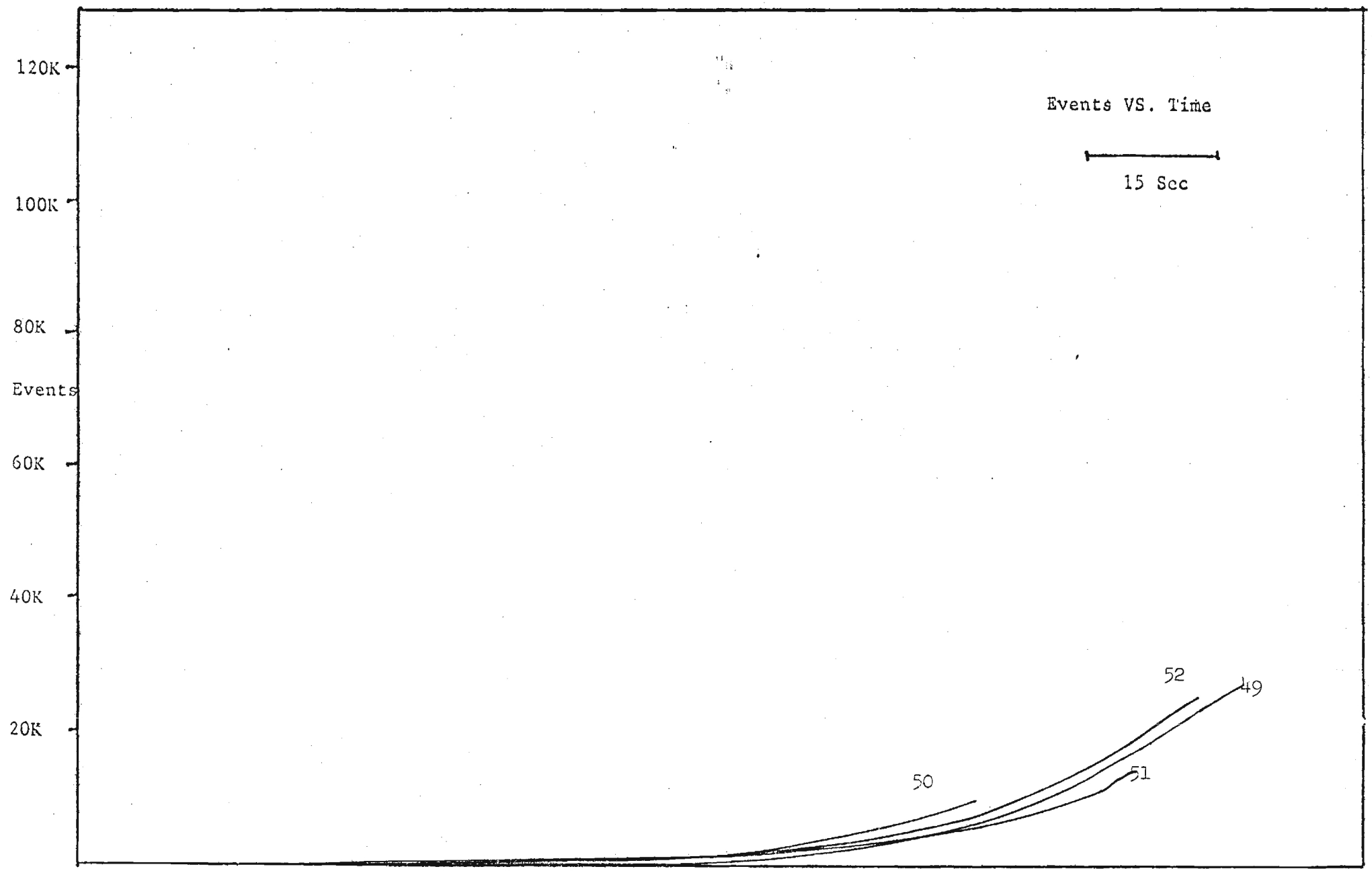

Fig. 11 Acoustic emission events for composite of tri-directional weave

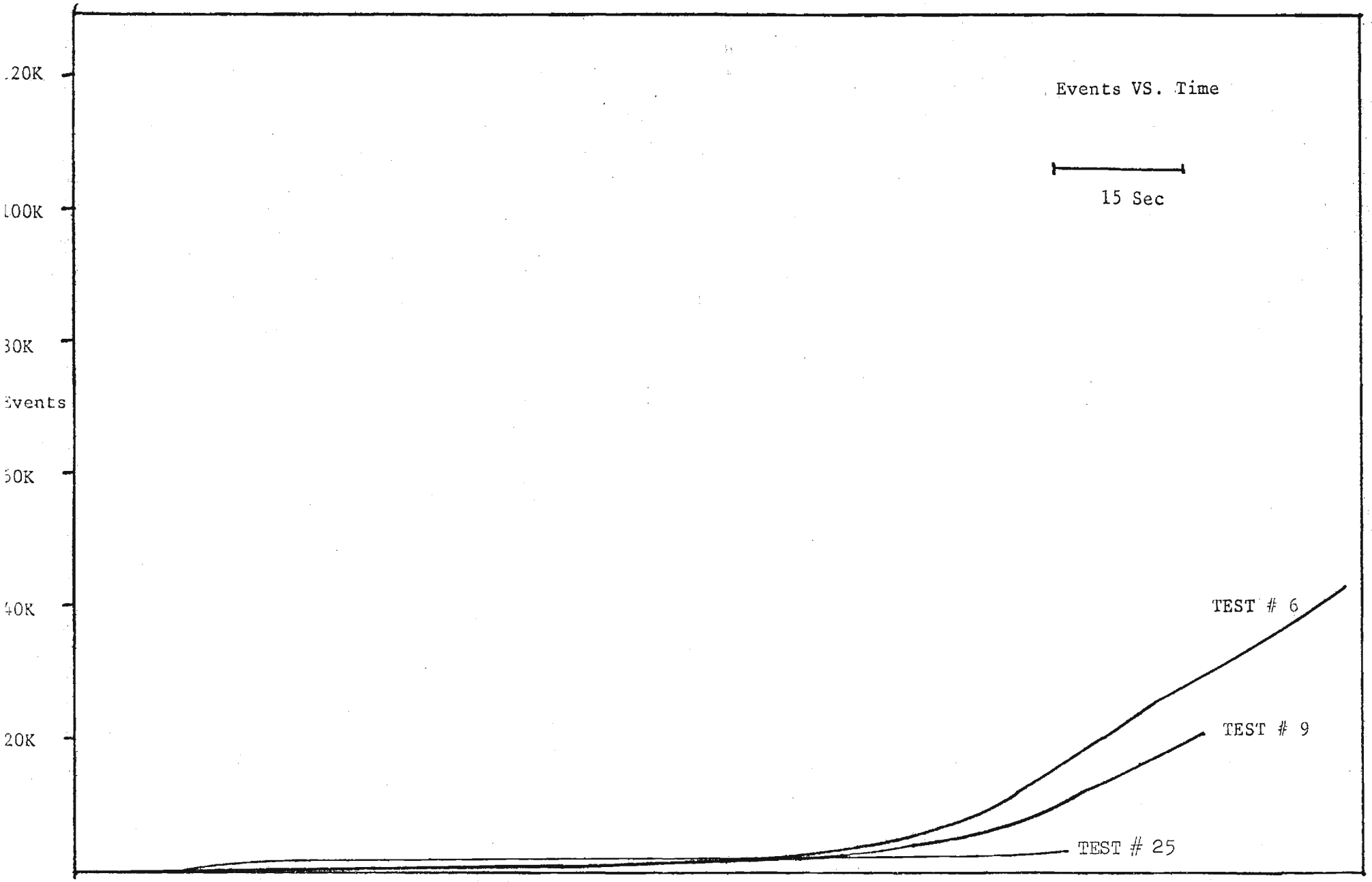

Fig. 12 Acoustic emission events from 37% unidirectional composite

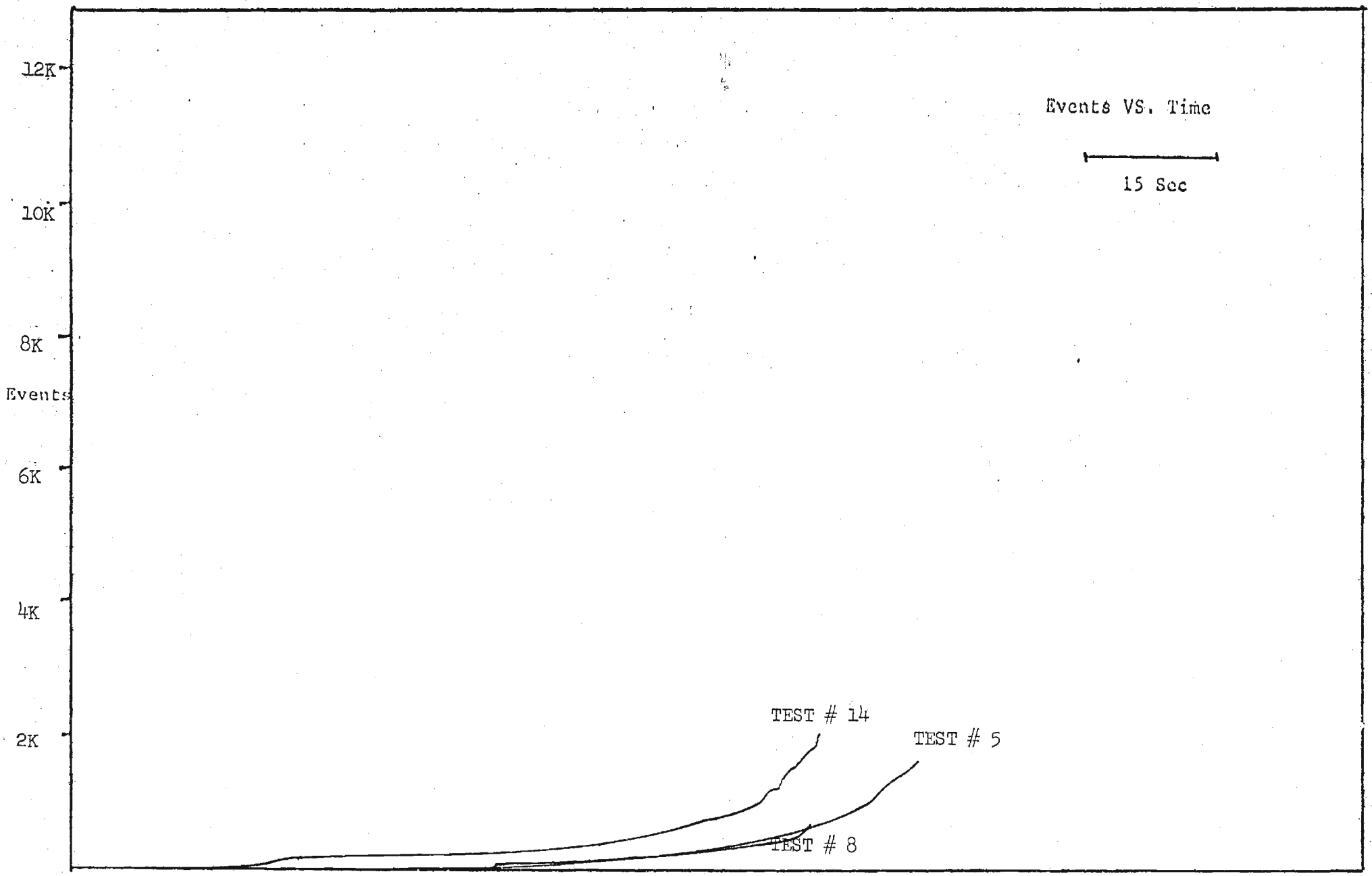

Fig. 13 Acoustic emission events for 50% unidirectional composites

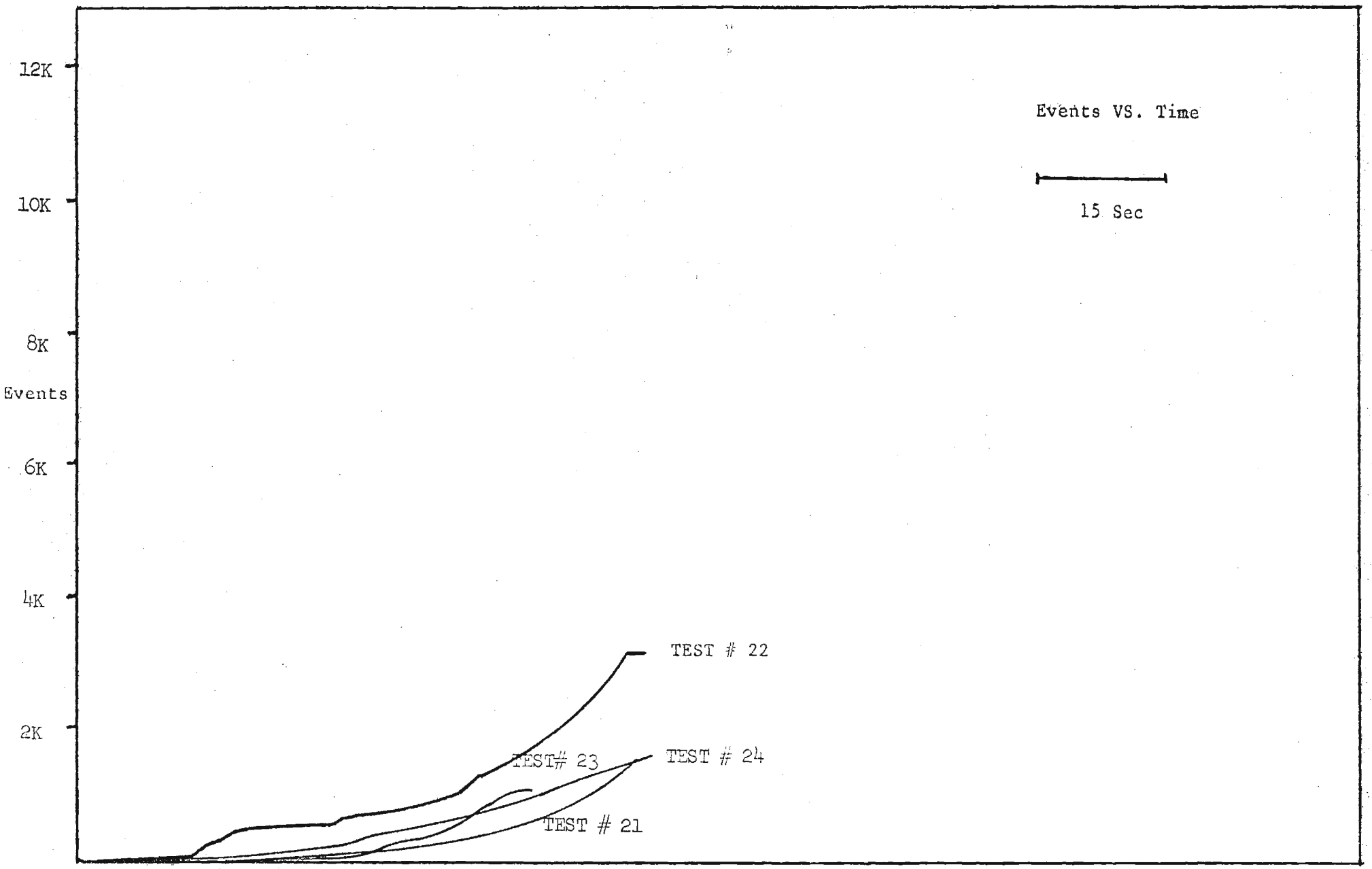

Fig. 14 Acoustic emission events for composite with holes

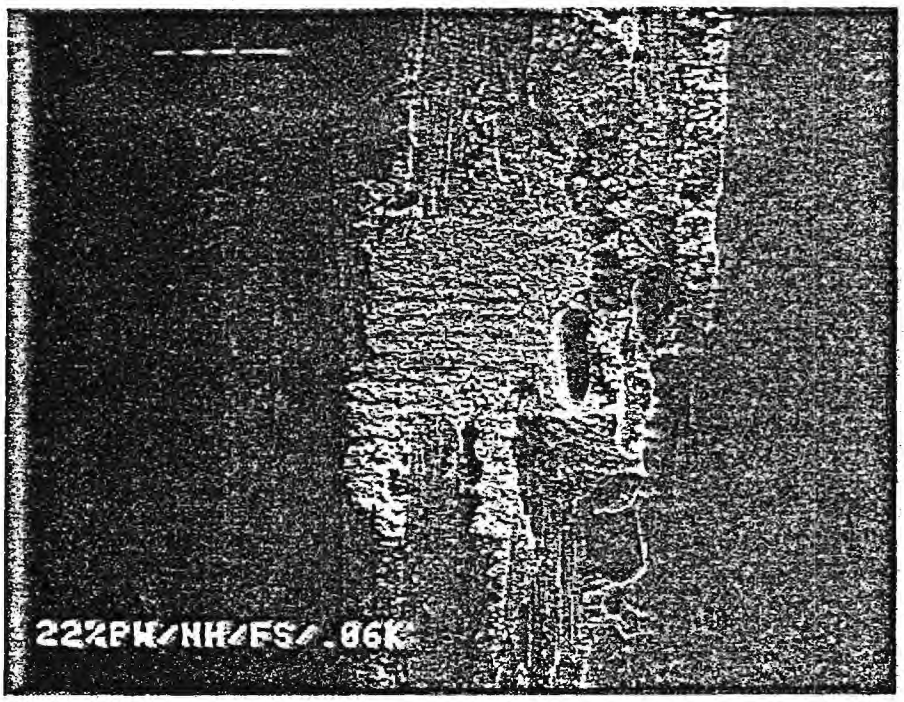

Fig. 15 Fractograph at 60 X

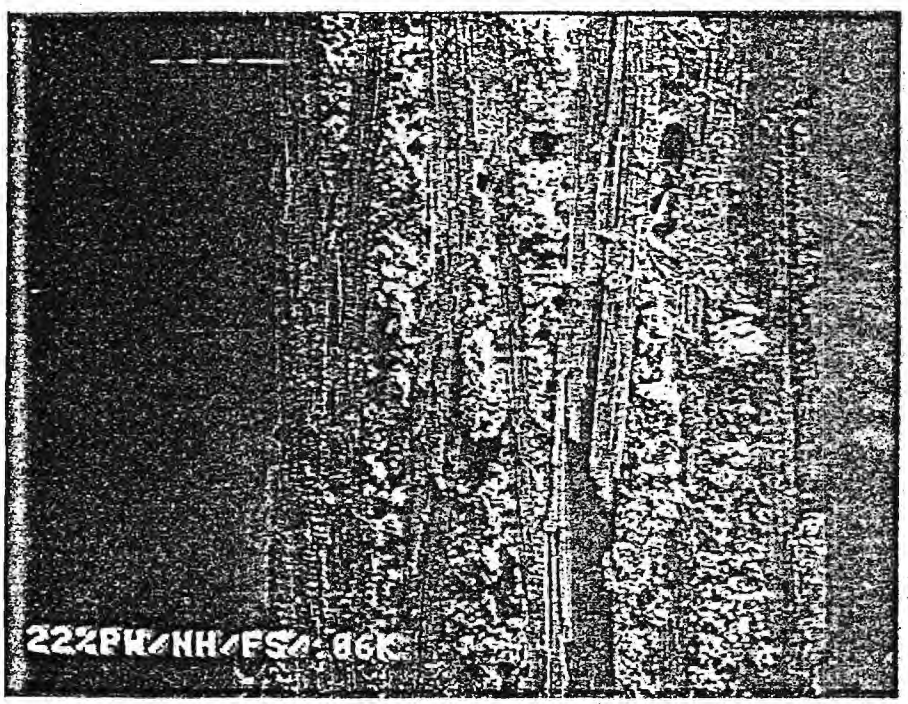

Fig. 16 Fractograph at 60 X

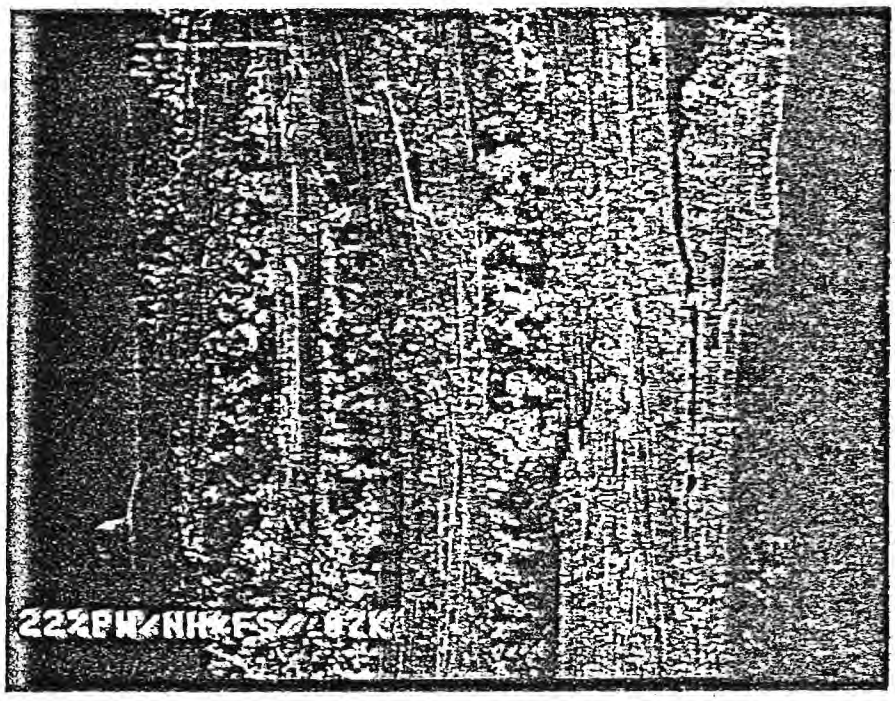

10

Fig. 17 Fractograpf at 70 X

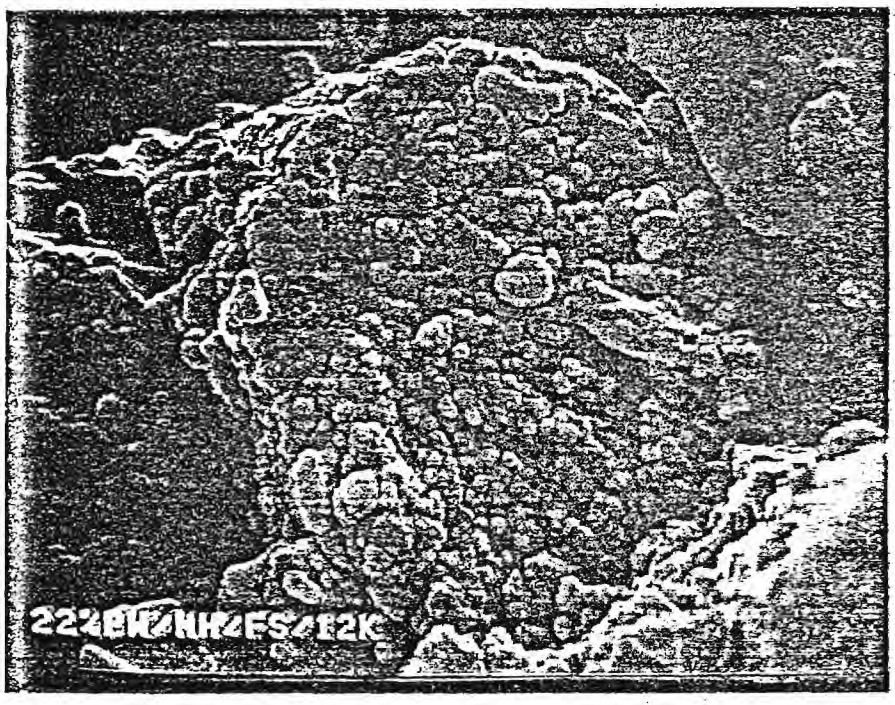

5

Fig. 18 Fractograph at 12000 X

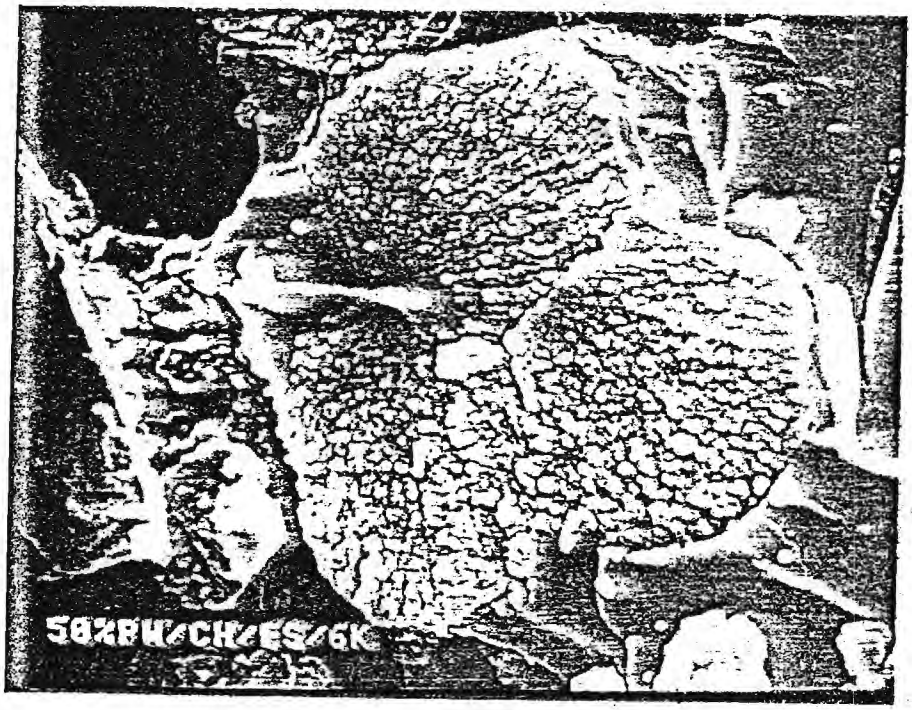

Fig. 19 Fractograph at 6000 X

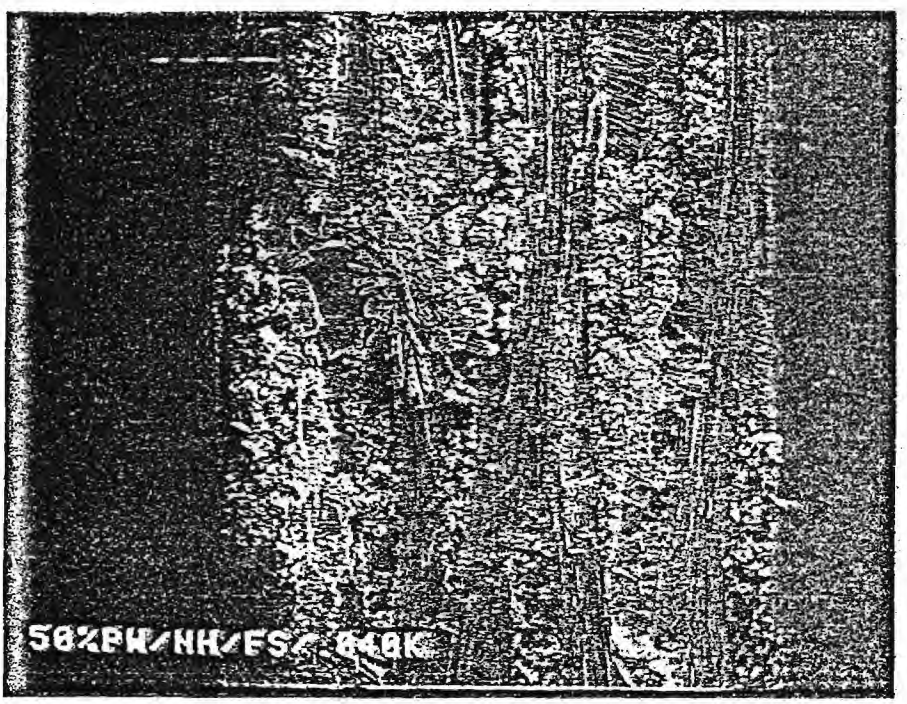

Fig. 20 Fractograph at 48 X

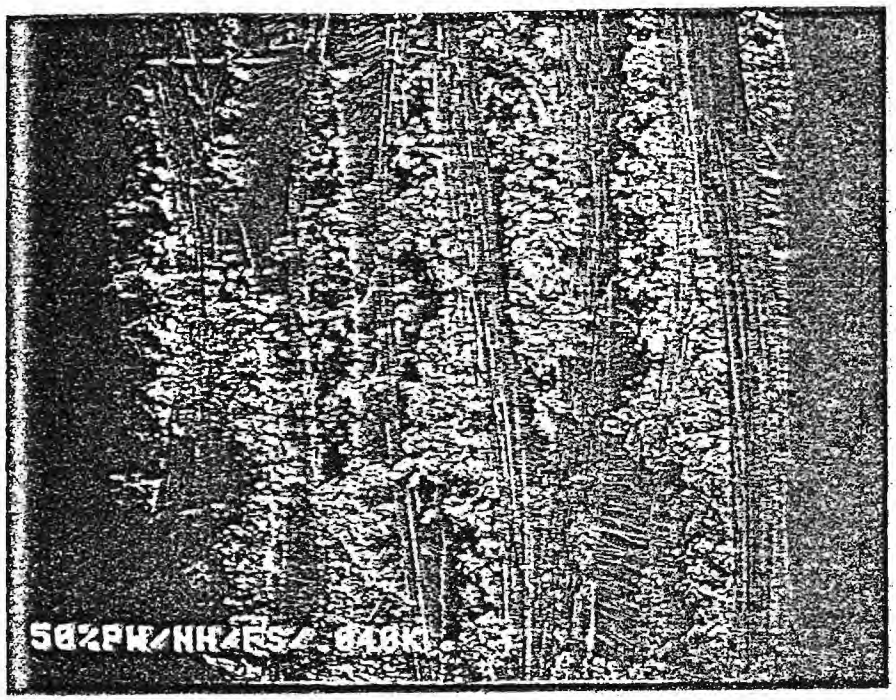

Fig. 21 Fractograph at 48 X

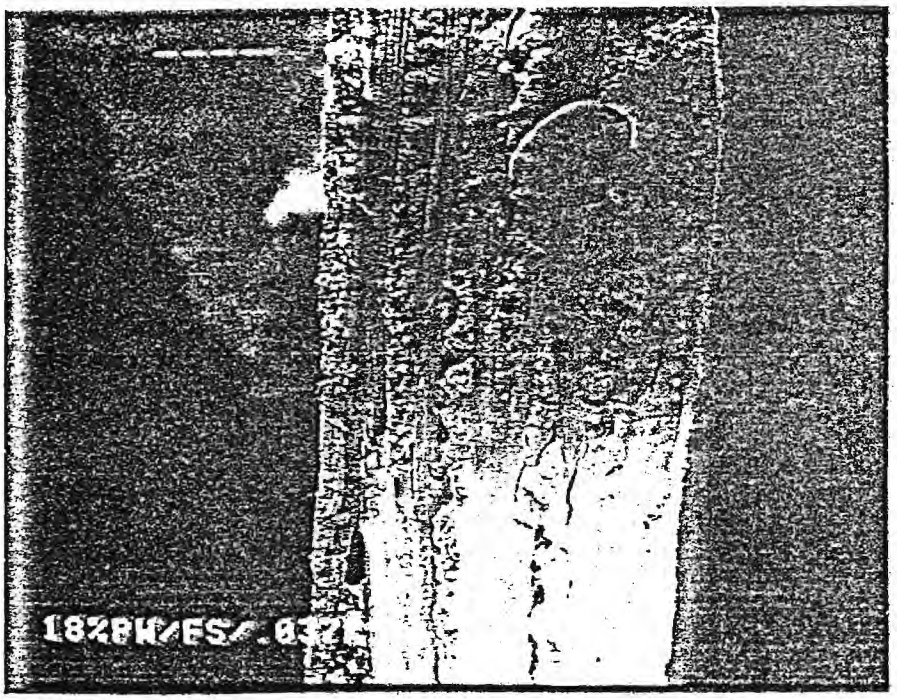

Fig. 22 Fractograph at 37 X

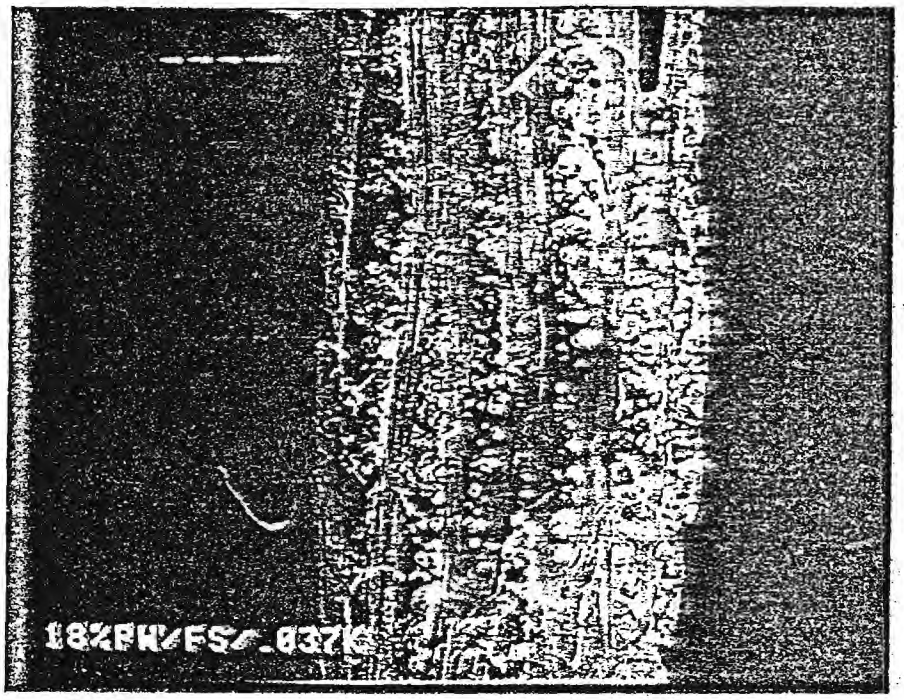

Fig. 23 Fractograph at 37 X

Fig. 24 Fractograph at 37 X

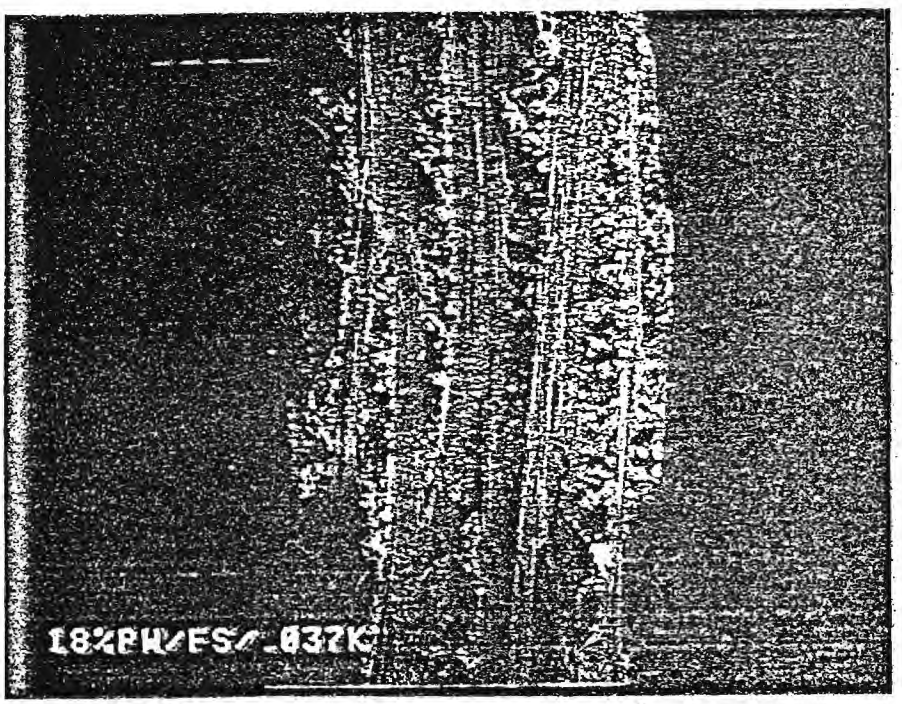

3

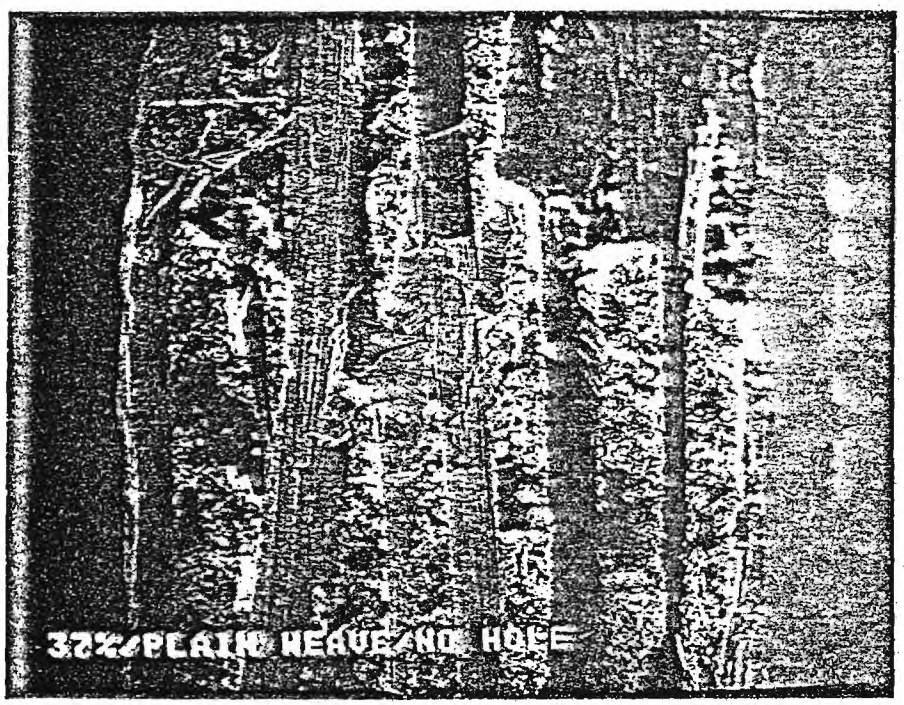

Fig. 24a Fractograph

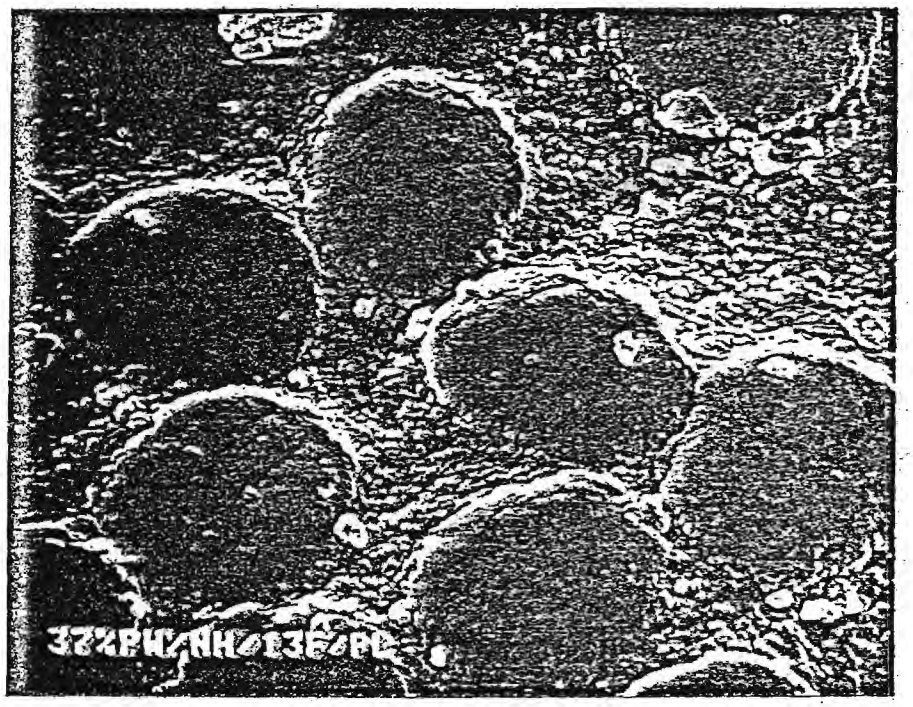

Fig. 25 Photomicrograph at 4700X

Fig. 26 Photomicrgraph at 4700 X

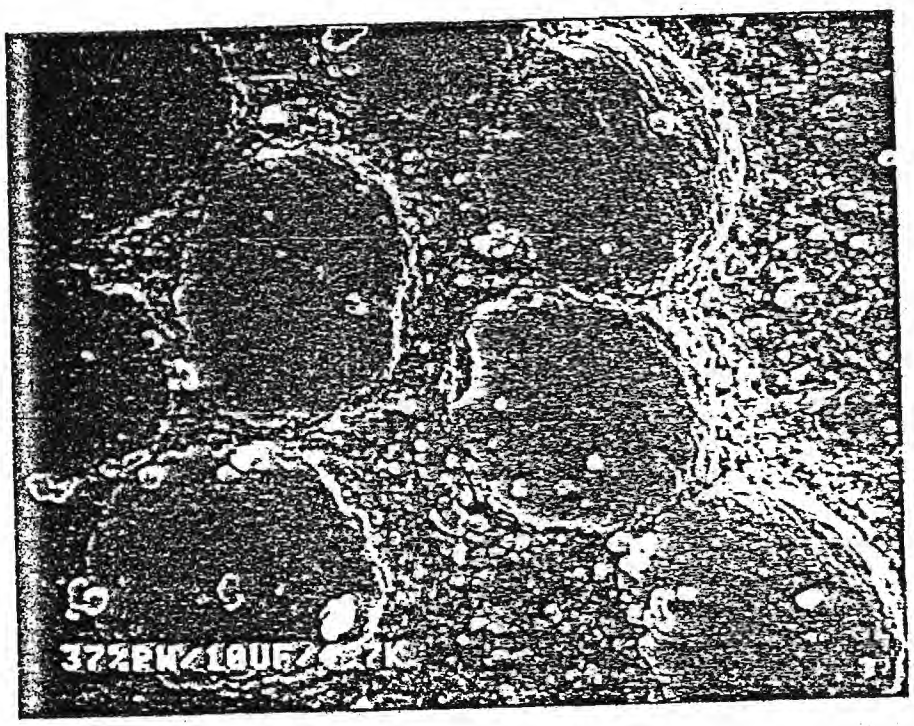

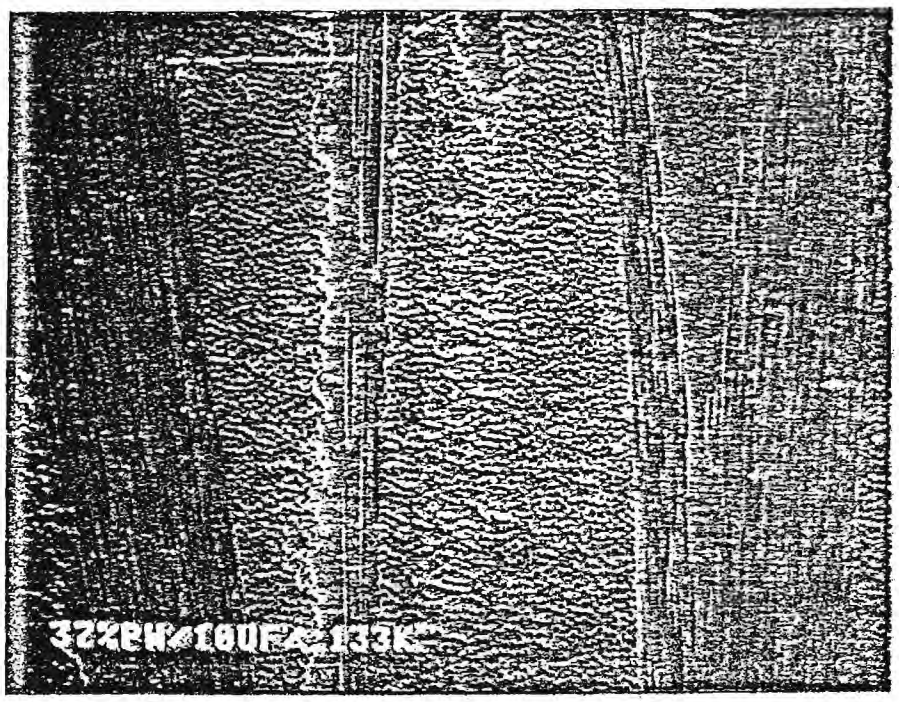

Fig. 27 Photomicrograph at 133 X

Fig. 28 Photomicrograph at9700 X

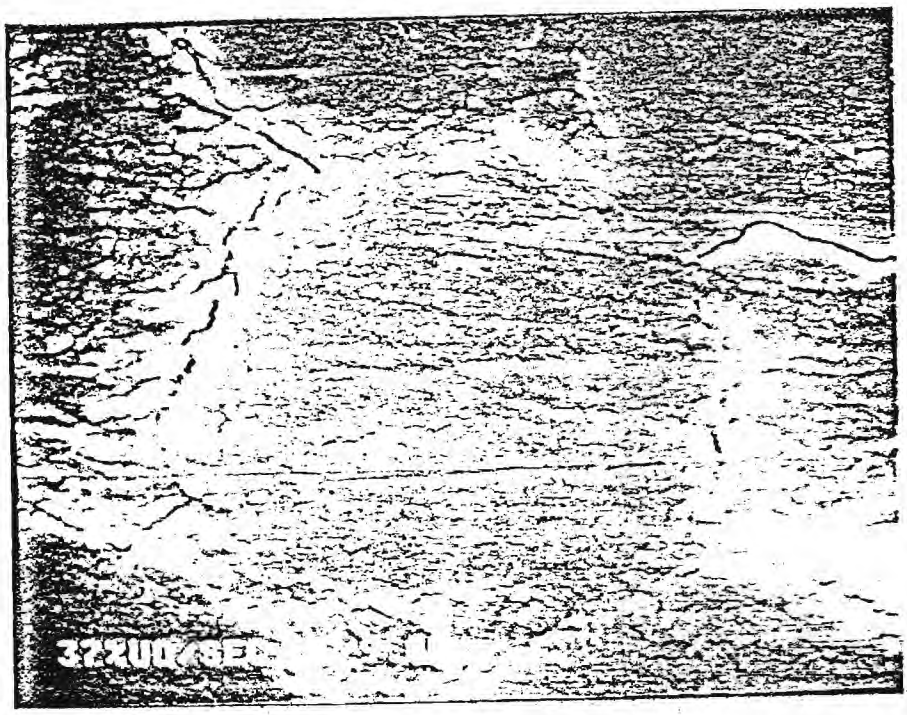

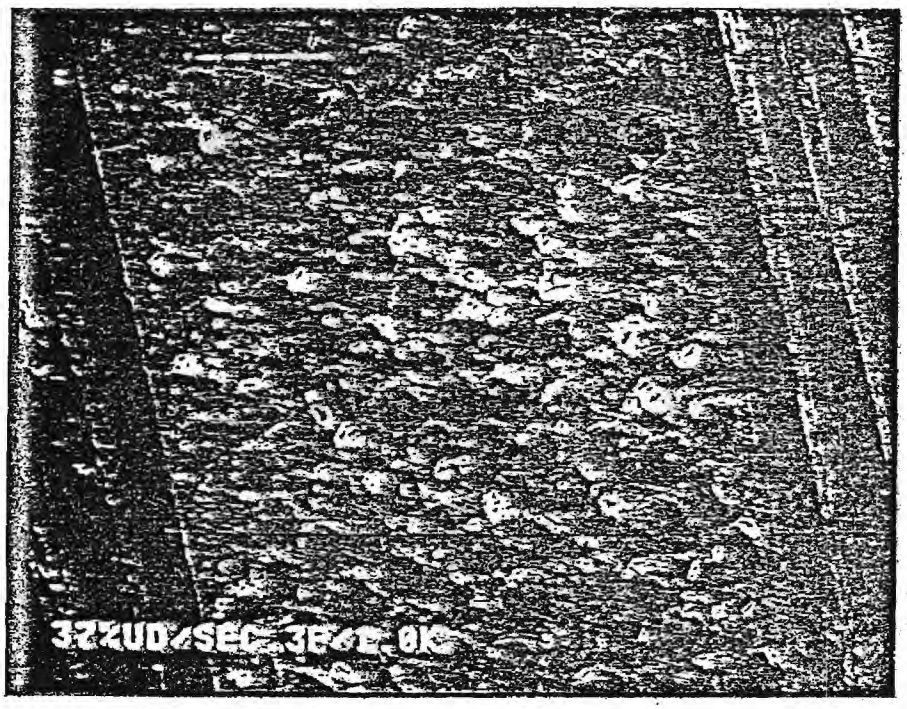

Fig. 29 Photomicrograph at 1000 X

Fig. 30 Photomicrograph at 1000 X

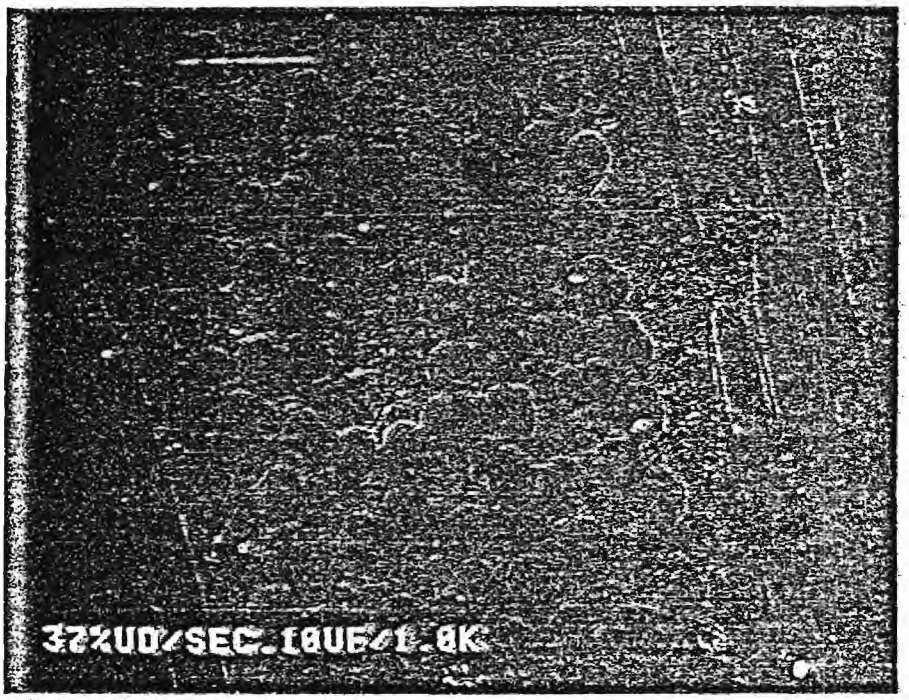

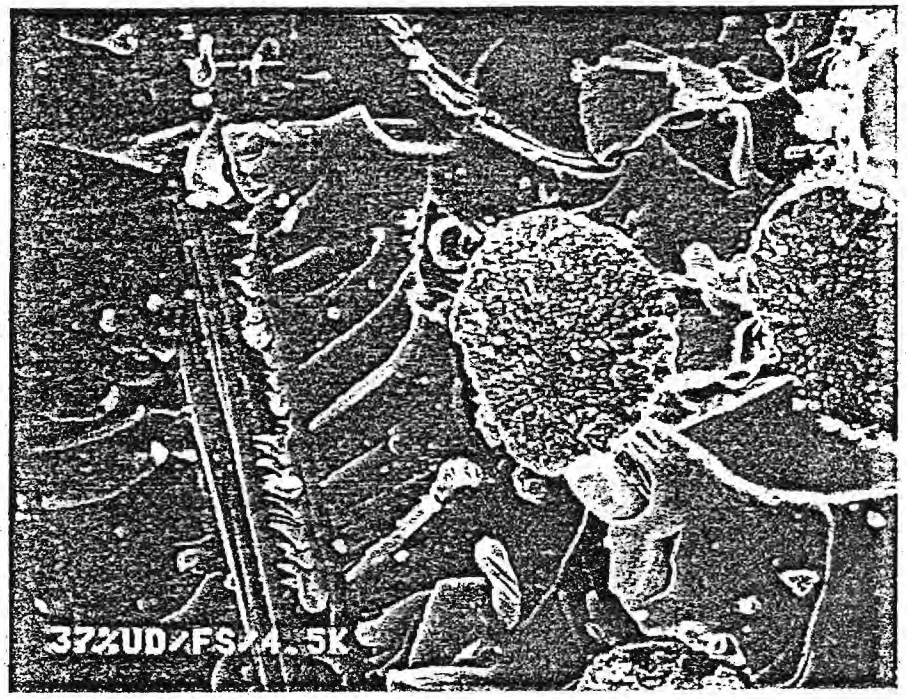

Fig. 31 Fractograph at 4500 X

Fig. 32 Fractograph at 43 X

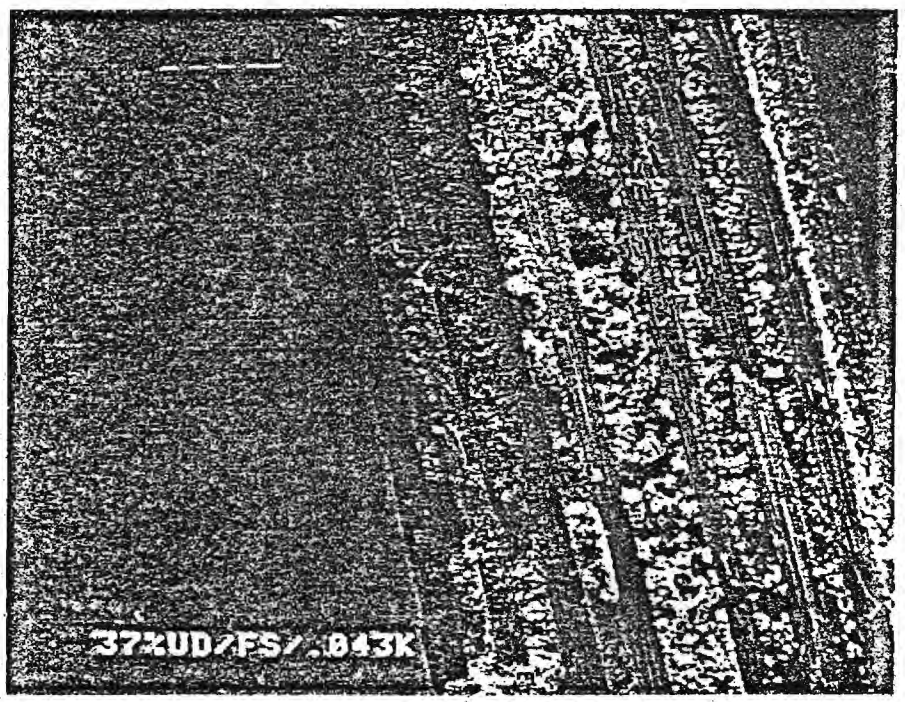

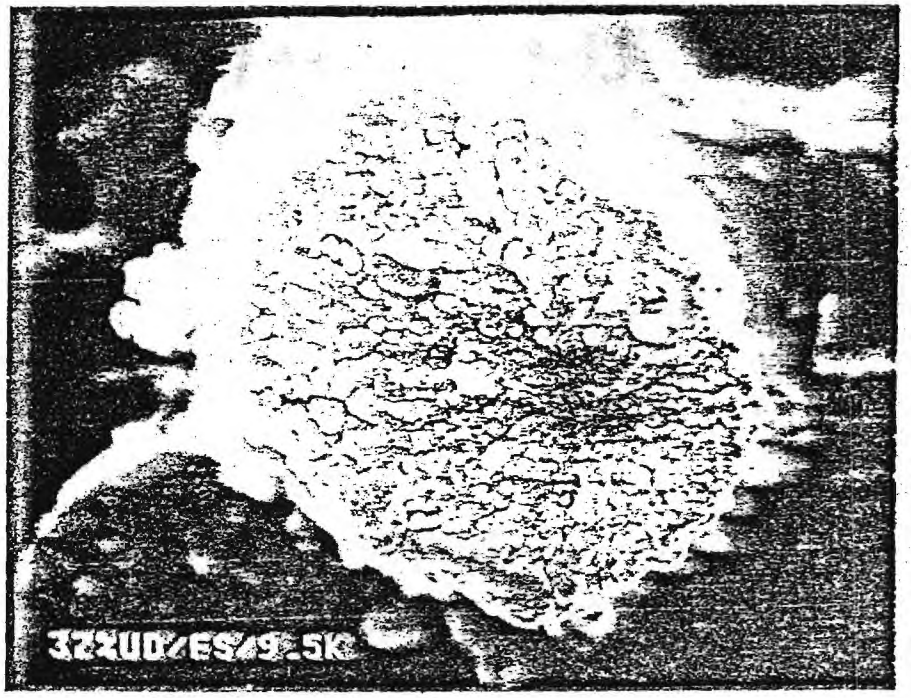

Fig. 33 Fractograph at 9500 X

Fig. 34 Fractograph at 18000 X

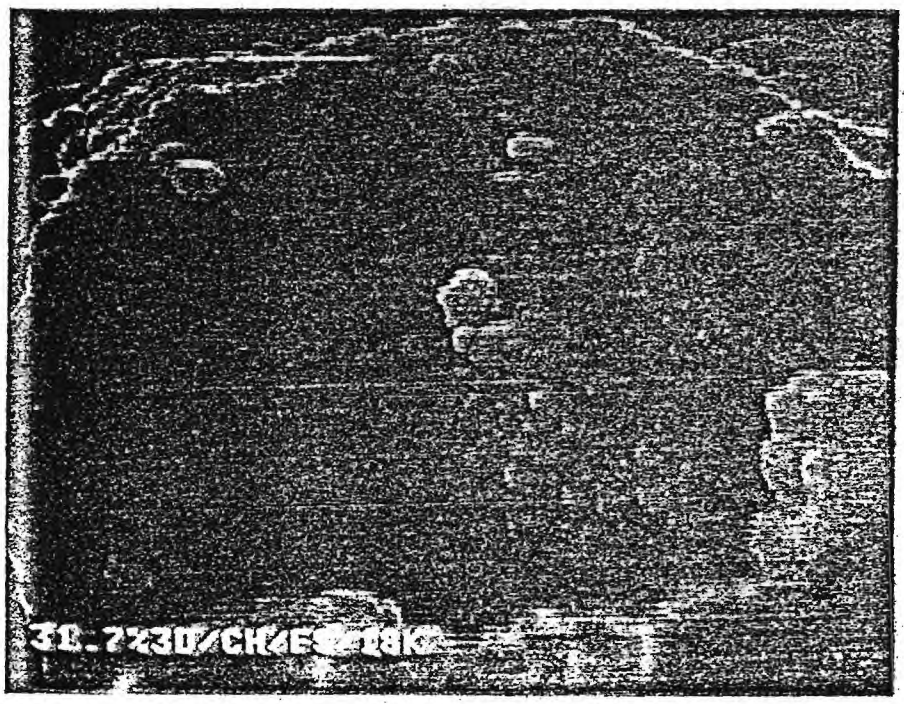

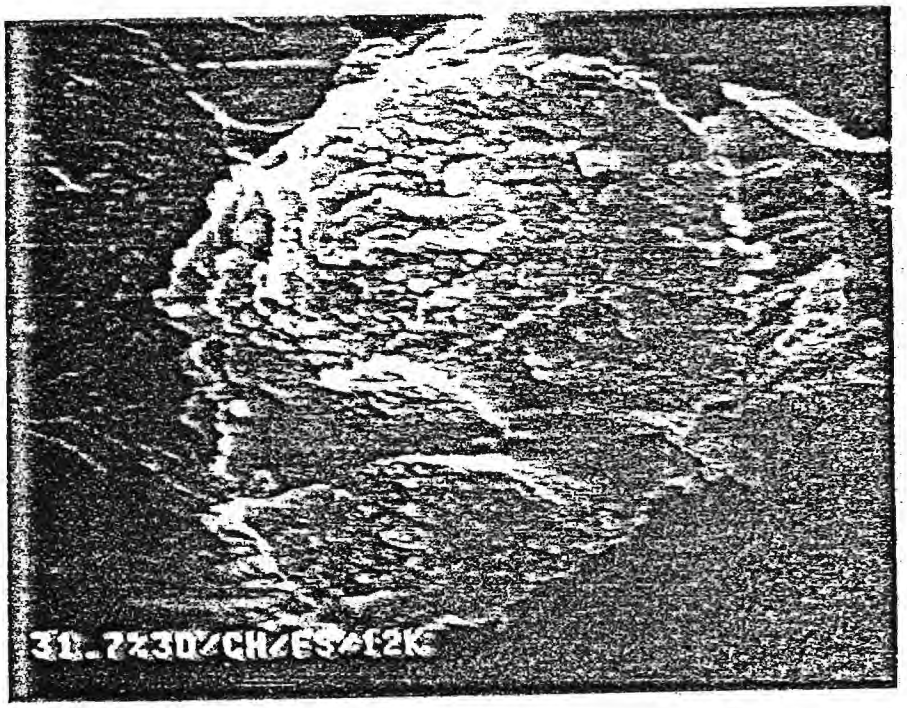

Fig. 35 Fractograph at 12000 X

Fig. 36 Fractograph at 3000 X

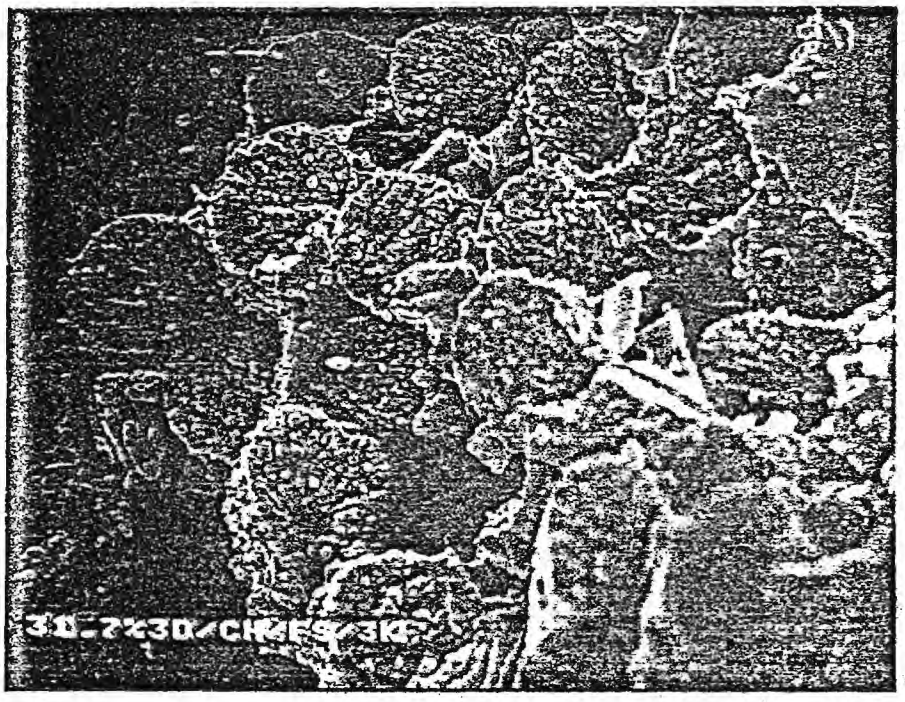

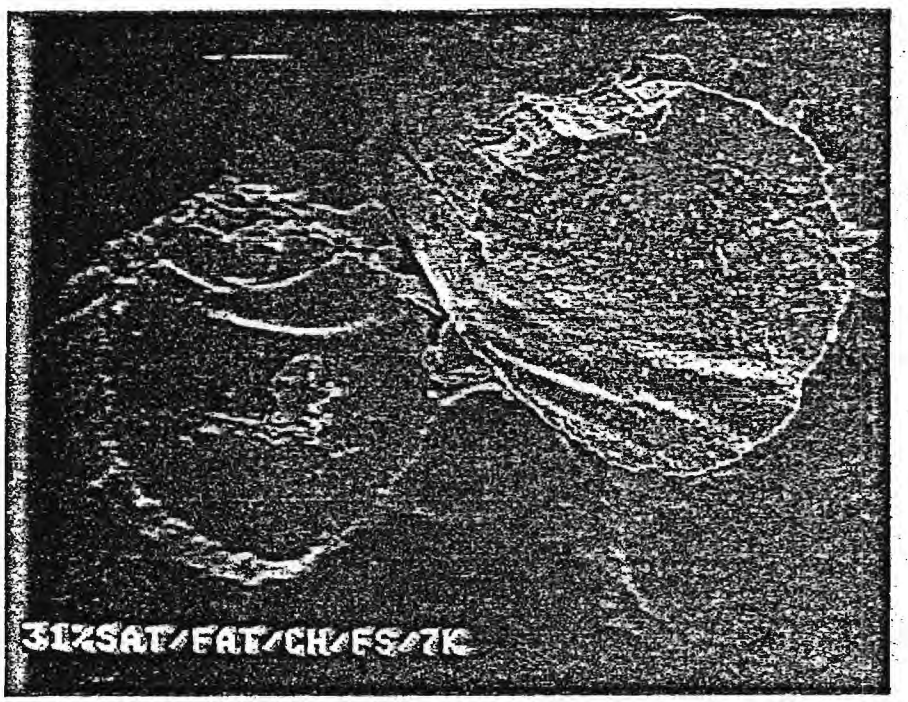

Fig. 37 Fractograph at 7000 X

Fig. 38 Fractograph at 7000 X

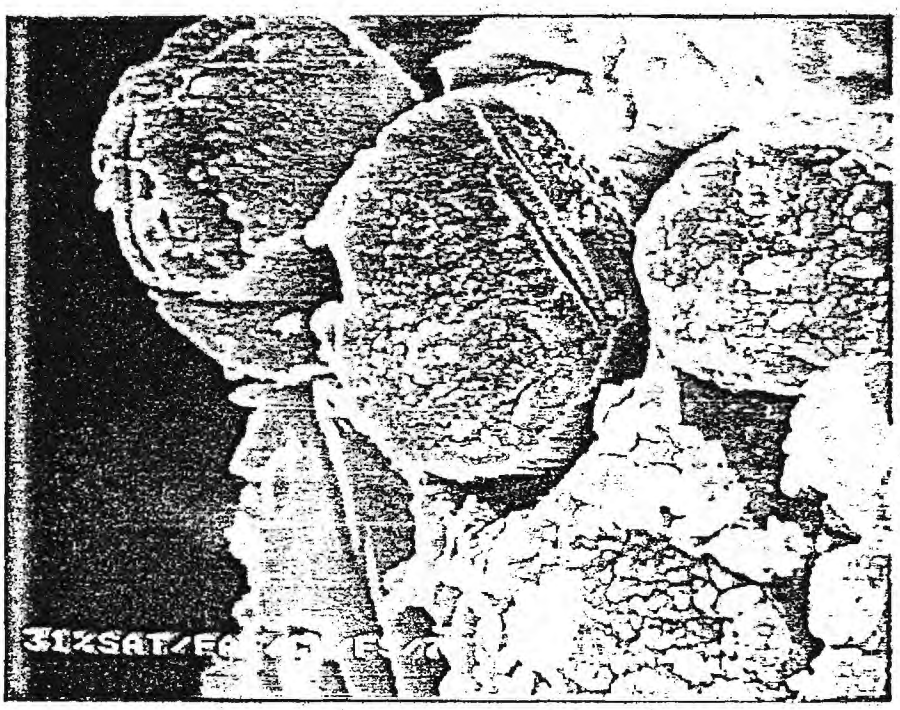

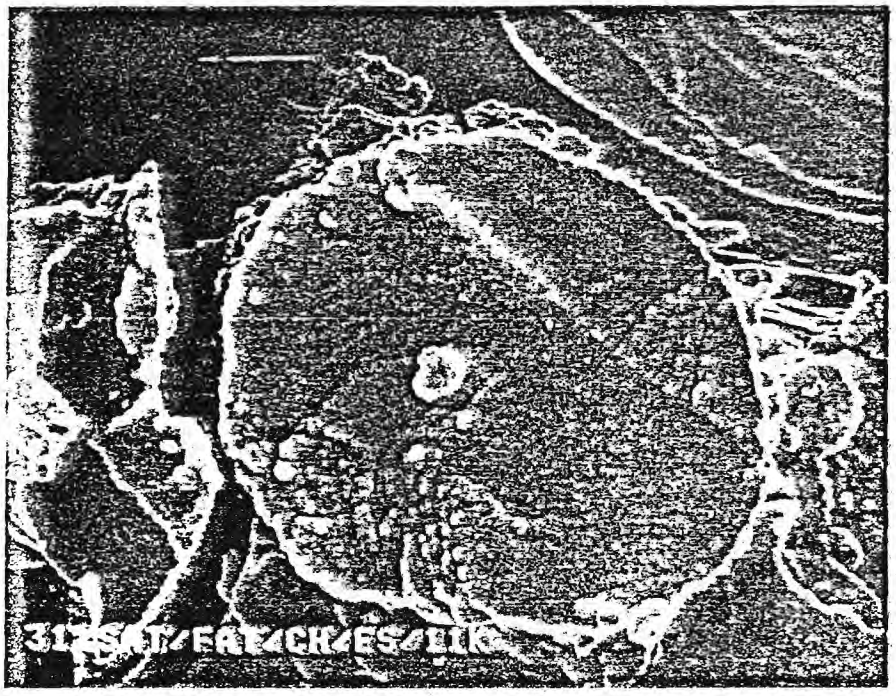

Fig. 39 Fractograph at 11000 X

Fig. 40 Fractograph at 2000 X

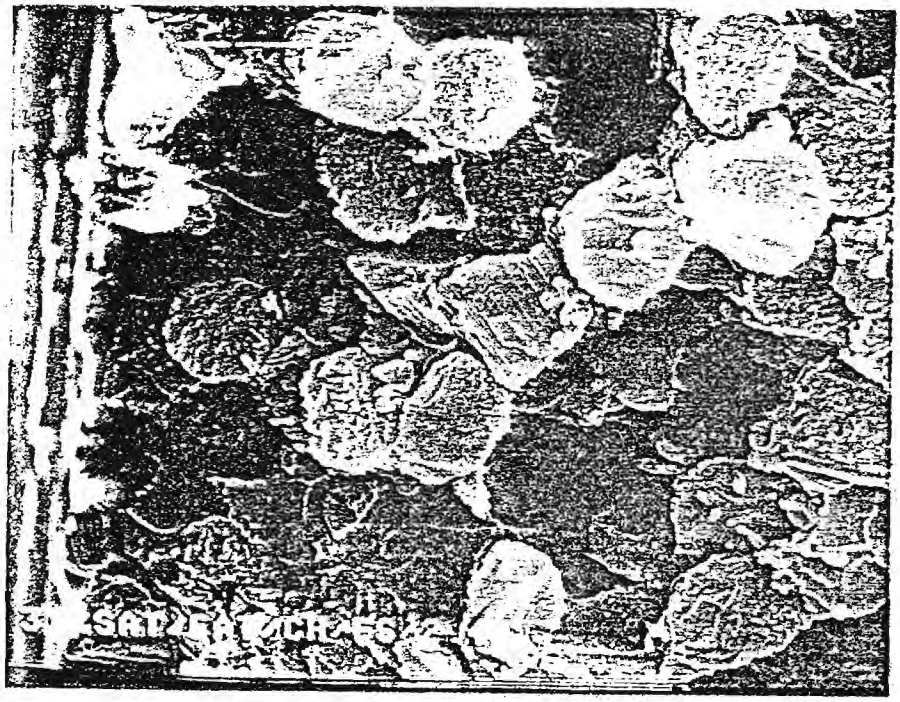

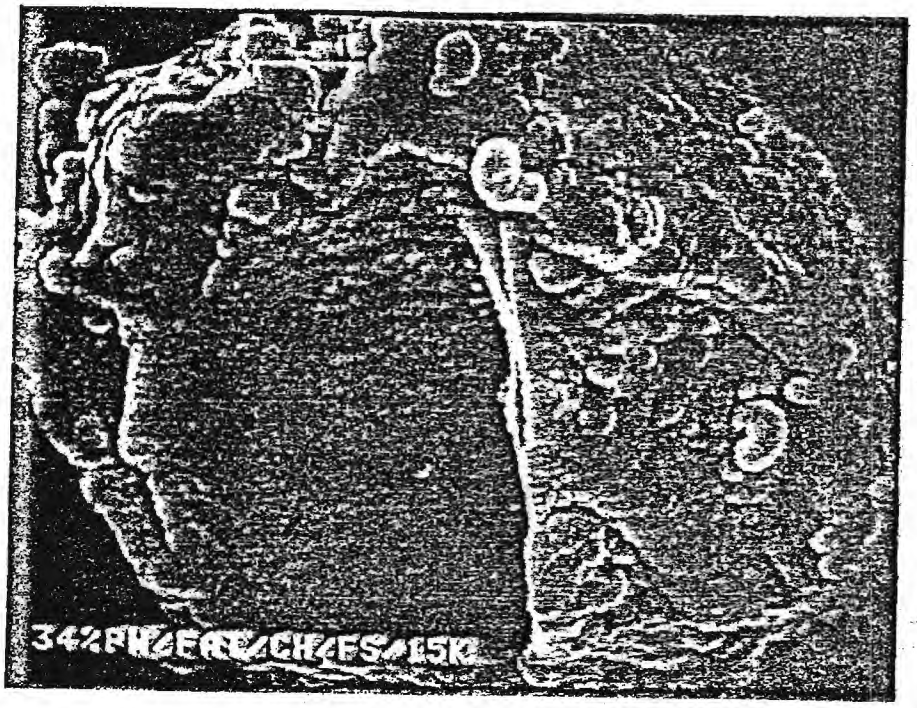

Figc 41 Fatigue Fractograph at 15000 X

Fig. 42 Fatigue Fractograph at 2500 X

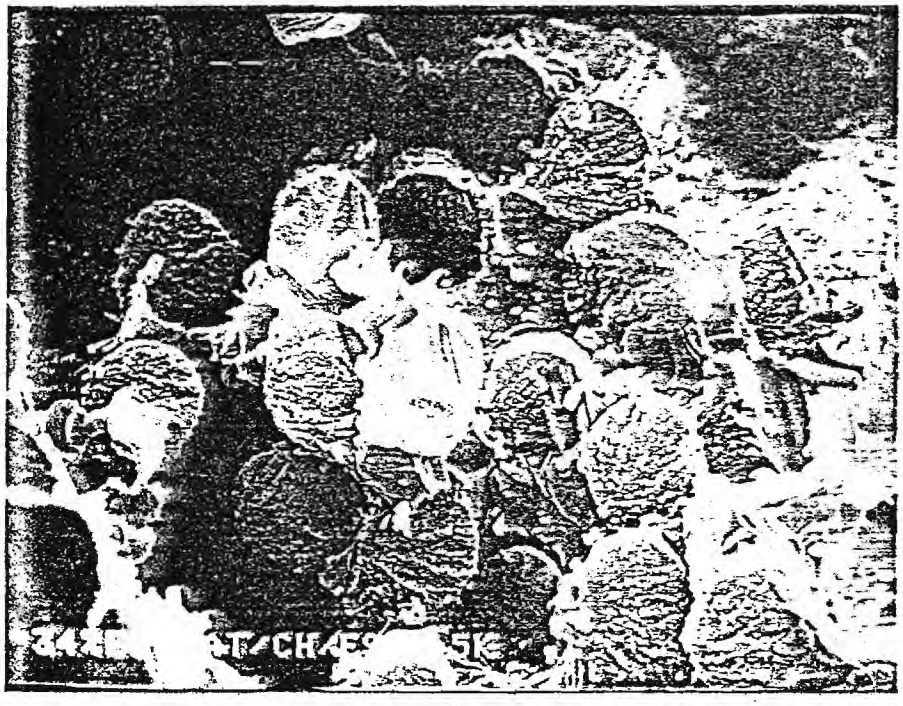

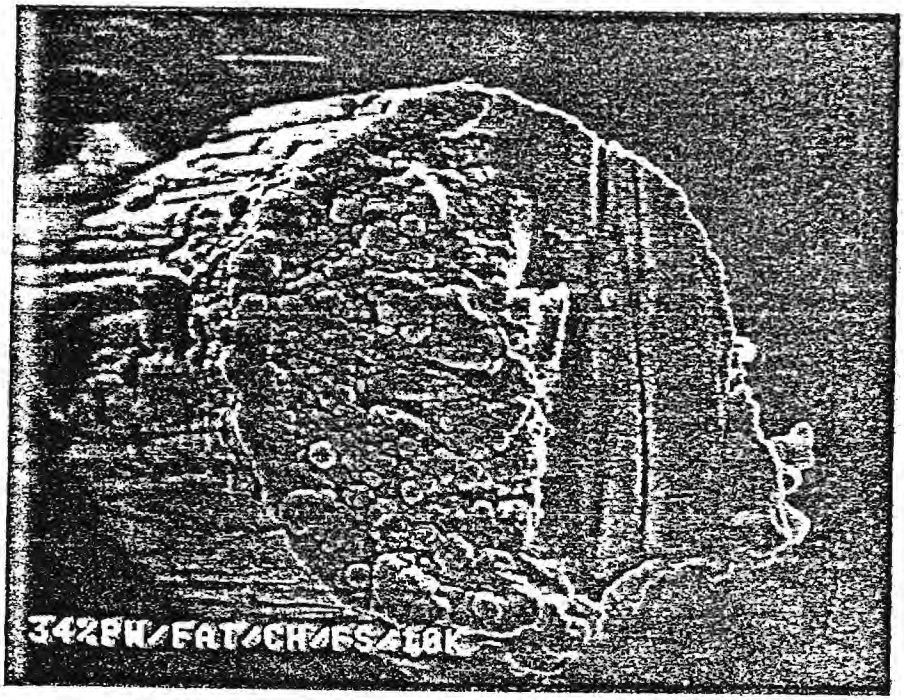

Fig. 43 Fatigue Fractograph at 10,000 X

Fig. 44 Fatigue Fractograph at 2500 X